Microscopic theory of diffraction of light from a small hole

Jesper Jung and Ole Keller*

Institute of Physics, Aalborg University, Skjernvej 4A, DK-9220 Aalborg Øst, Denmark

(Received 15 April 2014; revised manuscript received 24 September 2014; published 17 October 2014)

On the basis of the Maxwell-Lorentz local-field equations and nonlocal linear response theory, a self-consistent microscopic Green function theory of diffraction of light from a single hole in a thin and plane metallic screen is established. By subtracting the scattering of identical incident fields from screens with and without a hole, a causal effective optical aperture response tensor is introduced. An approximate expression is derived for the aperture response tensor in the limit where the screen behaves like an electric-dipole absorber and radiator. In this limit the internal electron dynamics is that of a quantum well. For a screen so thin that its bound electron motion can be described by a single quantum level, a approach for a quantum mechanical calculation of the aperture response tensor is presented. When the linear dimensions of the hole become sufficiently small the so-called aperture field, defined as the difference between the prevailing electric field with and that without a hole, becomes identical to the field from an incident-field-induced electric dipole with anisotropic linear polarizability. Our theory is formulated in such a manner that preknowledge only of (i) the incident electromagnetic field and (ii) the light-unperturbed optical electron properties (the microscopic conductivity tensor) of the screen with the geometrically given hole is needed. Since the microscopic theory allows for the presence of an (oscillating) component of the sheet current density perpendicular to the plane of the screen, a generalization of (i) the standard jump conditions of the field across the sheet and (ii) the reflection symmetries of the various fields in the plane of the screen is worked out. As our theory deviates radically from the approach of all classical diffraction theories, which are based on the macroscopic Maxwell equations and some kind of phenomenological expression for the screen conductivity σ (often just $\sigma \to \infty$), we give a brief review of classical diffraction theory, formulated in such a manner that a comparison to the microscopic theory is made easier. In particular, the Bethe-Bouwkamp theory of classical diffraction from a small hole in an infinitely thin and perfectly conducting ($\sigma \to \infty$) screen is our focus. We suggest that experimental frequency and angular resolved studies of the interference of the diffracted fields from quantum wells with and without holes are undertaken to obtain detailed insight into the microscopic aperture response functions, not least in the optical near-field domain.

DOI: 10.1103/PhysRevA.90.043830 PACS number(s): 42.25.Fx, 03.50.Kk

I. INTRODUCTION

A survey of the literature indicates that theoretical studies of the vectorial diffraction of electromagnetic fields (e.g., light) at an aperture (hole) in a metallic screen up to now have been based on the *macroscopic Maxwell equations*, together with the *standard boundary conditions*. Additionally, in the overwhelming majority of (older) investigations it is assumed that *the metal is a perfect conductor* (has infinite conductivity) and that *the screen is infinitely thin*. Classical theories invoking the latter two assumptions traditionally have been named rigorous diffraction theories [1], not for physical reasons but because the scattering problem becomes a well-defined mathematical boundary value problem. Although the perfect conductor assumption certainly is an idealization, it may represent a good approximation, particularly at electromagnetic frequencies far below optical frequencies. "Rigorous" classical diffraction studies most often start from the exact Helmholtz-Kirchhoff integral theorem [2–4] and proceed via the Kirchhoff method, in which the correct diffracted field in the hole is replaced by the incident field (possibly plus the reflected field), and the field behind the screen is assumed to vanish [1]. The Kirchhoff solution (scalar or vectorial) does not satisfy the boundary condition on the screen, however [5,6].

In an important paper [7] published in 1944, Bethe seeked to repair the "boundary condition defect" of the vectorial Kirchhoff theory and showed that a solution, satisfying the macroscopic Maxwell equations and the boundary conditions everywhere, could be obtained for a circular hole with a radius small compared to the wavelength of the incoming electromagnetic wave. The Bethe paper leads to the conclusion that the diffracted far field may be represented as owing to the radiation of an electric and a magnetic dipole, both placed in the center of the small hole. Although it was shown by Bouwkamp in 1950 that the result of Bethe needs a correction in the near field of the aperture [8,9], Bethe's paper offered substantial new physical insight into classical diffraction problems.

More recently, the advent of the scanning near-field microscope [10,11] (and the development of near-field optics as such) and the discovery of so-called extraordinary optical transmission [12] have stimulated new research on diffraction of light from single apertures and periodic hole arrays [13,14]. A good review of the extensive work in this field has been given by Garcia-Vidal *et al.* [15]. In 1987 Roberts presented a macroscopic classical diffraction theory of light from a circular aperture in a perfectly conducting screen of *finite* thickness using the so-called coupled-mode method [16]. Using a different approach, more along the lines of Bethe, the same geometry was analyzed by Garica de Abajo [17]. In the framework of the perfect conductor approximation

*okeller@physics.aau.dk

the coupled-mode method, moreover, has been used to study transmission of light through a rectangular hole [18] and to provide analytical expressions for transmittance through isolated circular and rectangular holes [19]. The spectral positions of the transmission resonances appearing in isolated holes also have been analyzed analytically using the coupled-mode method [20]. The diffraction of light from single apertures in nonideal metals, characterized by a complex dielectric constant, has been analyzed using different numerical methods to solve the related macroscopic Maxwell equations. Some of the first calculations were made by Wannermacher using the multiple-multipole method [21], but the Green's dyadic technique [22–26] and the finite-difference time-domain method [27] have also been employed. Recently a semianalytical approach for a circular subwavelength hole in a metal film was developed [28].

Partly motivated by the present authors' interest in understanding the *microscopic* physics related to the near-field diffraction of a single-photon wave packet (or a few photons) from a subwavelength hole, and single-photon near-field interference from two holes, we have found it necessary to reanalyze aspects of the electromagnetic diffraction theory starting from a quantum physical framework. As we see it, the description of a photon's transmission through a small hole cannot be separated from the spatial localization problem of the photon and this circumstance leads to the assertion that the photon tunneling effect, a genuine near-field quantum phenomenon, plays a crucial role in the vicinity of the hole [29]. The entire problem appears to be even more intriguing since there exists a link between near-field two-photon entanglement and spatial photon localization [30]. Due to the fact that a sufficiently small hole in the classical Bethe-Bouwkamp theory in the far field tends to behave like a source for electric- and magnetic-dipole radiation, a connection to certain theoretical quantum optical studies, in which the interference between the quantized electric-dipole (ED) radiation from two two-level atoms is examined, emerges [31,32].

As a forerunner to the full quantum electromagnetic theory, we present here a semiclassical microscopic theory, i.e., a description in which the electromagnetic field is treated as a classical quantity, whereas the massive particle (electron) dynamics is governed by the rules of quantum mechanics [the (many-body) Schrödinger equation].

In Sec. II, we give a summary of certain aspects of classical diffraction theory for perfect conductors, paying particular attention to a formulation adequate for a later comparison to our microscopic approach for a plane metallic screen. From the Lorenz-Rayleigh vectorial diffraction formula a bridge to the general scattering theory of the electromagnetic field from a current density sheet is made starting from the scattered vector potential in the Lorenz gauge. On the basis of the diffraction formula of Smythe [33], valid for the electric field of an infinitely thin and perfectly conducting screen, we calculate the diffracted field at distances from the aperture which are large compared to the linear dimensions of the hole, assuming that the field in the aperture is known. A determination of the electromagnetic field in the aperture poses a difficult problem, whose basic framework is briefly reviewed in Appendix A using an approach based on the insertion of an appropriate fictitious magnetic current density distribution into the aperture region.

In Sec. III, the microscopic diffraction theory is established, starting from the *microscopic Maxwell-Lorentz equations* in the frequency (ω) domain. In these *all* electromagnetic properties of matter are described via the microscopic charge and current densities, and only the microscopic electric and magnetic fields appear. From the outset, our approach deviates radically from the various classical ones in that we consider the determination of the *local microscopic electric field* [$\mathbf{E}(\mathbf{r};\omega)$] *inside* the screen to be the cental goal. The field-matter interaction generates a microscopic current density [$\mathbf{J}(\mathbf{r},\omega)$] in the screen. Under the assumption that this interaction is linear, $\mathbf{J}(\mathbf{r},\omega)$ and $\mathbf{E}(\mathbf{r};\omega)$ are related via a *spatially nonlocal constitutive equation* involving the *microscopic conductivity tensor*, $\boldsymbol{\sigma}(\mathbf{r},\mathbf{r}',\omega)$. Despite its name, a formulation based on $\boldsymbol{\sigma}(\mathbf{r},\mathbf{r}',\omega)$ enables one to describe the diffraction not only from metal screens but also from dielectric and semiconductor screens. The microscopic Maxwell-Lorentz equations allow one to set up an inhomogeneous integral relation between $\mathbf{E}(\mathbf{r},\omega)$ and $\mathbf{J}(\mathbf{r};\omega)$. The kernel of the relation is the well-known standard dyadic Green function, $\mathbf{G}(\mathbf{r},\mathbf{r}';\omega)$, and when $\mathbf{J}=\mathbf{0}$, the electric field equals the incident field $\mathbf{E}^0(\mathbf{r};\omega)$, an assumed preknown quantity. By combining the Green function formalism and the constitutive relation we obtain a *causal, spatially nonlocal constitutive equation* between the current density induced in the screen and the incident electric field. The related causal conductivity tensor $\boldsymbol{\sigma}^{\mathrm{cau}}(\mathbf{r},\mathbf{r}';\omega)$ can be obtained from $\mathbf{G}(\mathbf{r},\mathbf{r}'\omega)$ and a knowledge of $\boldsymbol{\sigma}(\mathbf{r},\mathbf{r}';\omega)$, at least formally. Once the current density in the screen has been calculated, it is easy to determine the diffracted field everywhere in space.

It appears from the outline given above that the microscopic diffraction problem for a *given* screen, characterized by its linear electrodynamic properties and the form of the aperture(s), placed in a prescribed incident field, has been turned into a question of calculating the microscopic response tensor $\boldsymbol{\sigma}^{\mathrm{cau}}(\mathbf{r},\mathbf{r}'\omega)$. In principle, $\boldsymbol{\sigma}^{\mathrm{cau}}(\mathbf{r},\mathbf{r}'\omega)$ may be determined from a knowledge of ω and the (many-body) wave functions and related eigenenergies of the Schrödinger equation describing the field-unperturbed electronic states of the *screen with a given aperture(s)*. In general, it is a hopeless task to make a direct quantum mechanical calculation of $\boldsymbol{\sigma}^{\mathrm{cau}}(\mathbf{r},\mathbf{r}'\omega)$. However, it is intuitively clear that it is the electronic properties of the screen in the vicinity of the aperture (hole) which are of primary importance. To take advantage of this, we compare the diffraction (scattering) from screens with and without holes. Apart form the disturbance caused by the hole the two screens are assumed to possess identical electrodynamic properties. Let $\boldsymbol{\sigma}^{\mathrm{cau}}(\mathbf{r},\mathbf{r}'\omega)$ and $\boldsymbol{\sigma}^{\mathrm{cau}}_{\infty}(\mathbf{r},\mathbf{r}'\omega)$ denote the relevant microscopic conductivity tensors for screens with and without a hole, respectively. Provided the screens are excited by identical incident fields, $\mathbf{E}^0(\mathbf{r};\omega)$, the *difference* between the diffracted fields in the two situations relates directly to a quantum mechanical calculation of the conductivity tensor difference $\boldsymbol{\sigma}^{\mathrm{cau}}(\mathbf{r},\mathbf{r}';\omega)-\boldsymbol{\sigma}^{\mathrm{cau}}_{\infty}(\mathbf{r},\mathbf{r}';\omega)$. As the reader may know, comparison of diffractions from (ideal conducting) screens with and without a hole is central to Bethe's analysis [7]. Although the determination of $\boldsymbol{\sigma}^{\mathrm{cau}}-\boldsymbol{\sigma}^{\mathrm{cau}}_{\infty}$ effectively involves only the electron dynamics in the vicinity of the hole,

the quantum mechanical calculation is still difficult to carry through, in general.

In the spirit of classical Bethe-Bouwkamp diffraction theory we next assume that the screen is so thin that it behaves like an ED absorber and ED radiator sheet (ED-ED sheet). In this limit, only the integral $[\boldsymbol{\Delta}(\mathbf{r}_\parallel,\mathbf{r}'_\parallel;\omega)]$ of $\boldsymbol{\sigma}^{\rm cau}(\mathbf{r},\mathbf{r}';\omega) - \boldsymbol{\sigma}^{\rm cau}_\infty(\mathbf{r},\mathbf{r};'\omega)$ over the directions (z and z') perpendicular to the screen appears. This fact simplifies the quantum mechanical calculation considerably. Furthermore, when the screen becomes sufficiently thin it behaves like a quantum well (QW). For QWs without a hole, much is known concerning the internal electron dynamics and $\boldsymbol{\sigma}^{\rm cau}(\mathbf{r},\mathbf{r}';\omega) = \boldsymbol{\sigma}^{\rm cau}(\mathbf{r}_\parallel,\mathbf{r}'_\parallel,z,z';\omega)$ (see Refs. [34] and [35], and references therein). For an ED-ED sheet (screen) the aperture response tensor, $\boldsymbol{\Delta}(\mathbf{r}_\parallel,\mathbf{r}'_\parallel;\omega)$, hence becomes the central quantity. The range of $\boldsymbol{\Delta}(\mathbf{r}_\parallel,\mathbf{r}'_\parallel;\omega)$ determines the effective size of the "hole" (the geometrical hole size plus the depth of the optical surface response layer).

A final simplification occurs if the effective hole size is small compared to the characteristic length parameter of the incident field. In the lowest order only the integral of $\boldsymbol{\Delta}(\mathbf{r}_\parallel,\mathbf{r}'_\parallel;\omega)$ over $\mathbf{r}_\parallel$ and $\mathbf{r}'_\parallel$ appears, and the related response tensor $\boldsymbol{\Delta}(\omega)$, multiplied by $i\omega$, takes the role of an ED polarizability tensor of the small hole.

In the microscopic diffraction theory, not least for QW sheets, it is necessary to take into account that the field-induced oscillatory (ω) screen current density in general has a component perpendicular to the plane of the sheet. This is well known for QWs without apertures, and the related generalization of the jump (boundary) conditions for the electromagnetic field has been obtained previously [34]. We show that the jump of the microscopic aperture field across the screen fulfills the generalized jump conditions, and in Appendix B, we add an analysis giving further insight into the physics behind these conditions. In particular, the jump in the component of the electric field parallel to the given interface is focused on, because this jump occurs only when the sheet current density has a component, $\mathbf{J}_\perp$, perpendicular to the interface.

It is known from classical diffraction theory that the reflection symmetries of the **A**, **E**, and **B** fields in the plane of the screen play a crucial role in the calculation of the diffracted electromagnetic field (cf. the summary given in Sec. II). It is important therefore to establish the generalized symmetries (asymmetries) existing when $\mathbf{J}_\perp$ is nonvanishing. This is done in Appendix C. In Sec. IV, we present how we, from a theoretical standpoint and in the wake of the present microscopic theory, see a possible future interplay between theory and experiments in the optical region, in particular, in the case of subwavelength holes in QW screens. In Sec. V, we show how the aperture response tensor of a metallic (or semiconducting) screen, with electron dynamics dominated by the diamagnetic interaction, may be obtained for a sheet so thin that it behaves like a single-level QW. A recently established two-dimensional (2D) extinction theorem [36], used here in combination with an infinite metal/hole barrier model, is central for the calculation. For a single-level QW with electronic-point correlation the difference between $\boldsymbol{\sigma}^{\rm cau}(\mathbf{r},\mathbf{r}';\omega)$ and $\boldsymbol{\sigma}(\mathbf{r},\mathbf{r}';\omega)$ takes a particularly simple form in the first Born approximation.

II. CLASSICAL DIFFRACTION THEORY

Since our microscopic theory of diffraction by a (small) hole in a plane conducting screen deviates radically from the classical approach, we begin with a summary of the classical theory. We highlight those aspects of the theory which are of particular importance for a comparison to our microscopic description, and we point out deficiencies and self-contradictory features shown by all classical approaches, essentially.

A. Lorenz-Rayleigh vectorial diffraction formula

Let us assume that the scalar field $u(\mathbf{r};\omega)$, given here in the space ($\mathbf{r}$)–frequency (ω) domain, satisfies the free-space Helmholtz equation

$$\left(\nabla^2 + q_0^2\right)u(\mathbf{r};\omega) = 0, \tag{1}$$

where $q_0 = \omega/c_0$ is the vacuum wave number of light (c_0 being the vacuum speed of light). A scalar Green function, $g(\mathbf{r},\mathbf{r}';\omega)$, for the Helmholtz equation is defined by

$$\left(\nabla^2 + q_0^2\right)g(\mathbf{r},\mathbf{r}';\omega) = -\delta(\mathbf{r}-\mathbf{r}'), \tag{2}$$

where $\delta(\mathbf{r}-\mathbf{r}')$ is the Dirac δ function. The Green function is not specified completely by Eq. (2), but for what follows it is adequate to make the choice

$$g(|\mathbf{r}-\mathbf{r}'|;\omega) = \frac{e^{iq_0|\mathbf{r}-\mathbf{r}'|}}{4\pi|\mathbf{r}-\mathbf{r}'|}. \tag{3}$$

The Green function in Eq. (3) is the so-called Huygens scalar propagator. If V is the volume bounded by a closed surface S and $\mathbf{r}$ is inside V, then [1,6,37]

$$u(\mathbf{r}) = \oint_S [u(\mathbf{r}')\hat{\mathbf{n}}(\mathbf{r}')\cdot\nabla' g(R) - g(R)\hat{\mathbf{n}}(\mathbf{r}')\cdot\nabla' u(\mathbf{r}')]dS', \tag{4}$$

where $\hat{\mathbf{n}}(\mathbf{r}')$ is the inwardly directed normal to S at point $\mathbf{r}'$. In the notation above the reference to ω has been left out, and $R = |\mathbf{R}| = |\mathbf{r}-\mathbf{r}'|$. Equation (4), which expresses the scalar field at $\mathbf{r}$ in terms of a surface integral over a certain surface S, is the integral theorem of Helmholtz and Kirchhoff [2–4]. To investigate the diffraction from an aperture in an infinitely thin plane screen (placed at $z = 0$) we let part of the surface of integration consist of the plane $z' = 0^+$. The remaining part of S is a hemisphere $\mathcal{S}_\infty$ in the half-space $z > 0$ (see Fig. 1). In the limit where the radius of the hemisphere is infinite, only the integral over the plane surface (henceforth denoted S) contributes. The integral over S therefore now extends over the screen $\mathcal{S}$ and the aperture $\mathcal{A}$, i.e., $S = \mathcal{S} + \mathcal{A}$. Other diffraction formulas equivalent to the one given in Eq. (4) are often used. For the present purpose it is useful to start from the Lorenz-Rayleigh integral formula

$$u(\mathbf{r}) = -2\int_{\mathcal{S}+\mathcal{A}} g(R)\frac{\partial u(\mathbf{r}')}{\partial z'}dS', \quad z > 0, \tag{5}$$

valid for diffraction from a plane screen (at $z = 0$) in the half-plane $z > 0$. The primary source of the incident scalar field, $u_0(\mathbf{r})$, must be located entirely in the region $z < 0$ for Eq. (5) to hold. The expression in Eq. (5) is generally known as the Rayleigh diffraction formula of the second kind [1], but

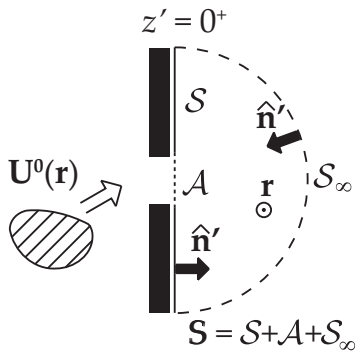

FIG. 1. Helmholtz-Kirchhoff integral theorem applied to investigate the diffraction of an incident vector field $\mathbf{U}^0(\mathbf{r})$ from an aperture in a plane screen. The surface is divided into three parts: the screen $\mathcal{S}$ (solid line) and the aperture $\mathcal{A}$ (short-dashed line) in the $z = 0^+$ plane and the remaining hemisphere $\mathcal{S}_\infty$ (dashed line). Note that $\mathbf{r}$ is a point inside S and that the normals $\hat{\mathbf{n}}' = \hat{\mathbf{n}}(\mathbf{r}')$ to the surface are inwardly directed.

we prefer to call it the Lorenz-Rayleigh diffraction formula because it is a fact that it was established by Lorenz in 1860 [38–40], many years before Rayleigh's independent 1897 publication [41].

For a vector field $\mathbf{U}(\mathbf{r}) = (u_x, u_y, u_z)$, where each of the Cartesian components satisfies the free-space Helmholtz equation, one obviously obtains the following vectorial equivalent of Eq. (5):

$$\mathbf{U}(\mathbf{r}) = -2\int_{\mathcal{S}+\mathcal{A}} g(R)\frac{\partial \mathbf{U}(\mathbf{r}')}{\partial z'}dS', \quad z > 0. \tag{6}$$

In the context of electromagnetism, one may, e.g., identify $\mathbf{U}$ with the vector potential ($\mathbf{A}$), the electric field ($\mathbf{E}$), or the magnetic field ($\mathbf{B}$). A number of other vectorial diffraction integrals equivalent to the one in Eq. (6) exists [1], but none of these is needed here. An incident vector field, $\mathbf{U}^0(\mathbf{r})$ (with sources located in the region $z < 0$), gives rise to a scattered field, $\mathbf{U}^S(\mathbf{r})$, from the screen, and the total field, $\mathbf{U}(\mathbf{r})$, prevailing in source-free points of space is hence

$$\mathbf{U}(\mathbf{r}) = \mathbf{U}^0(\mathbf{r}) + \mathbf{U}^S(\mathbf{r}). \tag{7}$$

The linearity of the free-space Maxwell equations allows one to apply Eq. (6) to $\mathbf{U}^0$, $\mathbf{U}^S$, or $\mathbf{U}$; cf. the vectorial Helmholtz wave equation. Before proceeding, we stress that Eq. (6) allows one to determine $\mathbf{U}(\mathbf{r})$ for $z > 0$ provided that $\partial\mathbf{U}(\mathbf{r}')/\partial z'$ in the $z = 0^+$ plane is known.

B. Remarks related to general scattering theory

Assume that an incident vector potential $\mathbf{A}^0(\mathbf{r};\omega) \equiv \mathbf{A}^0(\mathbf{r})$ interacts with a distribution of charged particles and (in a continuum description) gives rise to an induced current density $\mathbf{J}(\mathbf{r};\omega) \equiv \mathbf{J}(\mathbf{r})$ in the particle domain. In the Lorenz gauge the total vector potential, $\mathbf{A}(\mathbf{r};\omega) \equiv \mathbf{A}(\mathbf{r})$, is known to be given by the scattering formula [42]

$$\mathbf{A}(\mathbf{r}) = \mathbf{A}^0(\mathbf{r}) + \mu_0\int_{-\infty}^{\infty} g(R)\mathbf{J}(\mathbf{r}')d^3r', \tag{8}$$

where μ_0 is the vacuum permeability. Applied to an infinitely thin current sheet located in the plane $z = 0$, i.e., with $\mathbf{J}(\mathbf{r}) = \mathbf{J}^S(\mathbf{r}_\parallel)\delta(z)$ [where $\mathbf{r}_\parallel = (x,y)$], and under the assumption that $\mathbf{J}^S(\mathbf{r}_\parallel) = \mathbf{J}^S_\parallel(\mathbf{r}_\parallel) + \mathbf{J}^S_\perp(\mathbf{r}_\parallel)$ has no component perpendicular ($\perp$) to the plane of the sheet, that is,

$$\mathbf{J}^S_\perp(\mathbf{r}_\parallel) = \mathbf{0}, \tag{9}$$

the scattered vector potential $\mathbf{A}^S(\mathbf{r}) = \mathbf{A}(\mathbf{r}) - \mathbf{A}^0(\mathbf{r})$ is given by the surface integral

$$\mathbf{A}^S(\mathbf{r}) = \mu_0\int_{\mathcal{S}} g(R)\mathbf{J}^S_\parallel(\mathbf{r}'_\parallel)d^2r'_\parallel, \tag{10}$$

which only extends over the screen since $\mathbf{J}^S_\parallel(\mathbf{r}_\parallel) = \mathbf{0}$ in the aperture. Above and in the following the surface element $d\,S'$ over the screen is written as $d^2r'_\parallel$. Although all classical diffraction studies apparently have been based on the demand that the sheet current density in the screen must flow in directions parallel ($\parallel$) to the screen, i.e., $\mathbf{J}^S(\mathbf{r}_\parallel;\omega) = \mathbf{J}^S_\parallel(\mathbf{r}_\parallel;\omega)$, the requirement in general is correct only in the low-frequency limit $[\mathbf{J}^S(\mathbf{r}_\parallel;\omega \to 0) = \mathbf{J}^S_\parallel(\mathbf{r}_\parallel;\omega \to 0)]$ (cf. Refs. [34] and [35], and references therein). In our microscopic approach, we relax the assumption in Eq. (9).

In order to solve the macroscopic as well as the microscopic diffraction problem the boundary (jump) conditions for the electromagnetic field at the plane of the screen must be investigated. In Appendix B, we establish the boundary conditions in the general case where $\mathbf{J}^S_\perp(\mathbf{r}_\parallel,\omega) \neq \mathbf{0}$ and show that these reduce to the standard boundary conditions [6] for $\mathbf{J}^S_\perp(\mathbf{r}_\parallel,\omega) = \mathbf{0}$. We also derive the connection between a given scattered vector field ($\mathbf{A}^S$, $\mathbf{E}^S$, or $\mathbf{B}^S$) in the space points (x,y,z) and $(x,y,-z)$ in Appendix C. For $\mathbf{J}^S_\perp(\mathbf{r}_\parallel,\omega) = \mathbf{0}$ we regain the well-known (standard) reflection symmetries for the scattered vector field. Since the incident electromagnetic field is differentiable at every space point, the jump conditions refer to the scattered fields.

When $\mathbf{J}^S_\perp(\mathbf{r}_\parallel,\omega) = \mathbf{0}$, the component of the magnetic field parallel to the screen is odd in z. This fact, in combination with the standard jump condition for the magnetic field across a nonmagnetic current sheet, gives

$$2\hat{\mathbf{n}} \times \mathbf{B}^S(\mathbf{r}_\parallel, z = 0^+;\omega) = \mu_0\mathbf{J}^S_\parallel(\mathbf{r}_\parallel;\omega). \tag{11}$$

By inserting Eq. (11) into Eq. (10) one obtains

$$\mathbf{A}^S(\mathbf{r}) = 2\int_{\mathcal{S}} g(R)\hat{\mathbf{n}} \times \mathbf{B}^S(\mathbf{r}'_\parallel,0^+)d^2r'_\parallel. \tag{12}$$

In the two equations above $\hat{\mathbf{n}} = (0,0,1)$.

The result in Eq. (12) may be derived in a slightly different manner starting from Eq. (6) applied to the diffracted vector potential, viz.,

$$\mathbf{A}^S(\mathbf{r}) = -2\int_{\mathcal{S}+\mathcal{A}} g(R)\frac{\partial \mathbf{A}^S(\mathbf{r}'_\parallel,0^+)}{\partial z'}d^2r'_\parallel. \tag{13}$$

It appears from Eq. (10) that the vector potential is parallel to the plane of the screen, everywhere; that is, $\hat{\mathbf{n}} \cdot \mathbf{A}^S(\mathbf{r}) = 0$. Since $\mathbf{B}^S(\mathbf{r}) = \nabla \times \mathbf{A}^S(\mathbf{r})$, this in turn implies that

$$-\frac{\partial \mathbf{A}^S(\mathbf{r})}{\partial z} = \hat{\mathbf{n}} \times \mathbf{B}^S(\mathbf{r}). \tag{14}$$

With this relation inserted into Eq. (13) one is led back to Eq. (12).

C. Diffraction formula of Smythe: A perfectly conducting screen

An integral expression for the scattered magnetic field is obtained by taking the curl of Eq. (12). Hence,

$$\mathbf{B}^S(\mathbf{r}) = 2\nabla \times \int_{\mathcal{S}+\mathcal{A}} g(R)\hat{\mathbf{n}} \times \mathbf{B}^S(\mathbf{r}'_\parallel,0^+)d^2r'_\parallel, \quad z \neq 0, \tag{15}$$

in a notation where we formally have extended the surface integral to include the aperture region where $\hat{\mathbf{n}} \times \mathbf{B}^S(\mathbf{r}_\parallel,0^+) = \mathbf{0}$.

Since the duality transformation $\mathbf{E}^S \Rightarrow c_0\mathbf{B}^S$, $\mathbf{B}^S \Rightarrow -\mathbf{E}^S/c_0$ leaves the *free-space* Maxwell equations for the scattered field form invariant, a relation analogous to the one in Eq. (15) holds for the scattered electric field for $z > 0$, viz.,

$$\mathbf{E}^S(\mathbf{r}) = 2\nabla \times \int_{\mathcal{S}+\mathcal{A}} g(R)\hat{\mathbf{n}} \times \mathbf{E}^S(\mathbf{r}'_\parallel,0^+)d^2r'_\parallel, \quad z > 0. \tag{16}$$

The reflection symmetries for $\mathbf{E}^S$ in the $z = 0$ plane implies that the right-hand side of Eq. (16) must be multiplied by -1 for $z < 0$. The duality transformation also holds for the incident electromagnetic field, and therefore, starting from Eq. (6) applied to the incident vector potential, $\mathbf{A}^0$, a moment's thought shows that the incident electric field $\mathbf{E}^0(\mathbf{r})$ has an integral expansion

$$\mathbf{E}^0(\mathbf{r}) = 2\nabla \times \int_{\mathcal{S}+\mathcal{A}} g(R)\hat{\mathbf{n}} \times \mathbf{E}^0(\mathbf{r}'_\parallel,0^+)d^2r'_\parallel, \quad z > 0, \tag{17}$$

in the right half-space. By addition of Eqs. (16) and (17) one obtains

$$\mathbf{E}(\mathbf{r}) = 2\nabla \times \int_{\mathcal{A}} g(R)\hat{\mathbf{n}} \times \mathbf{E}(\mathbf{r}'_\parallel,0^+)d^2r'_\parallel, \quad z > 0. \tag{18}$$

As indicated, the surface integral only extends over the aperture because it has been assumed that *the infinitely thin metallic screen is a perfect conductor* (has infinite conductivity), so that the total electric field ($\mathbf{E}$) vanishes on the screen. The standard (textbook) boundary conditions for $\mathbf{E}$ thus yield $\hat{\mathbf{n}} \times \mathbf{E}(\mathbf{r}'_\parallel,0^+) = 0$ over the screen. The integral relation in Eq. (18) was first obtained by Smythe [33] in 1947 and later (in 1954) presented by Bouwkamp [9] in his review of diffraction theory.

In order to determine the diffracted electric field from Eq. (18) one needs preknowledge of the tangential electric field $\hat{\mathbf{n}} \times \mathbf{E}(\mathbf{r}_\parallel,z = 0^+)$ over the aperture. Since the electric field is continuous in the hole $\mathbf{E}(\mathbf{r}_\parallel,z = 0^-) = \mathbf{E}(\mathbf{r}_\parallel,z = 0^+)[=\mathbf{E}(\mathbf{r}_\parallel,0)] \equiv \boldsymbol{\mathcal{E}}(\mathbf{r}_\parallel)$. Once $\boldsymbol{\mathcal{E}}(\mathbf{r}_\parallel)$ has been determined (in practice, only approximately) the diffracted field can be determined everywhere in the half-space $z > 0$ from

$$\mathbf{E}(\mathbf{r}) = 2\nabla \times \int_{\mathcal{A}} g(|\mathbf{r} - \mathbf{r}'_\parallel|)\hat{\mathbf{n}} \times \boldsymbol{\mathcal{E}}(\mathbf{r}'_\parallel)d^2r'_\parallel, \quad z > 0, \tag{19}$$

by a direct integration over the aperture. The central problem in classical diffraction theory hence is the determination of the aperture field $\boldsymbol{\mathcal{E}}(\mathbf{r}_\parallel)$. In Appendix A, we indicate how the aperture-field problem has been addressed by introducing a *fictitious magnetic current density distribution* in the hole region (see also Refs. [5,7,9,33,43], and [44], and references therein). As noted by Smythe [33], Eq. (18) [or Eq. (19)] has the exact same form as the term from the integrated field equations used by Bethe [7] in his analysis of diffraction from a small circular hole. In Bethe's 1944 paper a certain approximate calculation of $\boldsymbol{\mathcal{E}}(\mathbf{r}_\parallel)$ was presented.

D. Diffracted field at "large" distances from the aperture

Let us now assume that we are interested in the electric field at distances from the aperture which are large compared to the linear extension of the aperture; i.e., $|\mathbf{r}| \gg |\mathbf{r}'_\parallel|$. From a Taylor expansion of the Huygens propagator around $\mathbf{r}$, viz.,

$$g(|\mathbf{r} - \mathbf{r}'_\parallel|;\omega) = \frac{e^{iq_0r}}{4\pi r} - \mathbf{r}'_\parallel \cdot \hat{\mathbf{r}}\frac{iq_0r - 1}{4\pi r^2}e^{iq_0r} + \ldots, \tag{20}$$

where $\hat{\mathbf{r}} = \mathbf{r}/r$, one finds that the diffracted field [Eq. (19)] in lowest (zeroth) order, $\mathbf{E}^{(0)}(\mathbf{r};\omega)$, is given by

$$\mathbf{E}^{(0)}(\mathbf{r};\omega) = \left(iq_0 - \frac{1}{r}\right)\frac{e^{iq_0r}}{2\pi r}\hat{\mathbf{r}} \times \int_{\mathcal{A}} \hat{\mathbf{n}} \times \boldsymbol{\mathcal{E}}(\mathbf{r}'_\parallel;\omega)d^2r'_\parallel. \tag{21}$$

Using the relation $\hat{\mathbf{r}} \times (\ldots) = \mathbf{U} \times \hat{\mathbf{r}} \cdot (\ldots)$, where $\mathbf{U}$ is the unit tensor, Eq. (21) may be rewritten in the form

$$\mathbf{E}^{(0)}(\mathbf{r};\omega)[\equiv\mathbf{E}^{\mathrm{MD}}(\mathbf{r};\omega)] = -\frac{\mu_0}{c_0}\omega^2\mathbf{G}_{\mathrm{M}}(\mathbf{r};\omega) \cdot \mathbf{m}(\omega), \tag{22}$$

where

$$\mathbf{G}_{\mathrm{M}}(\mathbf{r};\omega) = \frac{iq_0}{4\pi}\left(\frac{1}{iq_0r} - \frac{1}{(iq_0r)^2}\right)e^{iq_0r}\mathbf{U} \times \hat{\mathbf{r}} \tag{23}$$

is the so-called magnetic Green function [42]. The expression in Eq. (22) shows that the diffracted field to the lowest order in $r'_\parallel/r$ equals the electric field from a magnetic dipole [42] of moment,

$$\mathbf{m}(\omega) = \frac{2}{i\mu_0\omega}\hat{\mathbf{n}} \times \int_{\mathcal{A}} \boldsymbol{\mathcal{E}}(\mathbf{r}'_\parallel;\omega)d^2r'_\parallel. \tag{24}$$

It appears from this equation that the magnetic-dipole moment lies in the aperture plane. This is in agreement with the conclusion obtained by Bethe in the far field of a small circular aperture [7]. For the first-order term one gets

$$\begin{aligned}\mathbf{E}^{(1)}(\mathbf{r};\omega) &= -\frac{1}{2\pi}\nabla \times \int_{\mathcal{A}} (\mathbf{r}'_\parallel \cdot \hat{\mathbf{r}})\frac{iq_0r - 1}{r^2} \\ &\quad \times e^{iq_0r}\hat{\mathbf{n}} \times \boldsymbol{\mathcal{E}}(\mathbf{r}'_\parallel;\omega)d^2r'_\parallel \\ &= -\frac{1}{2\pi}\int_{\mathcal{A}} \nabla\left(\frac{iq_0r - 1}{r^2}e^{iq_0r}\mathbf{r}'_\parallel \cdot \hat{\mathbf{r}}\right) \\ &\quad \times [\hat{\mathbf{n}} \times \boldsymbol{\mathcal{E}}(\mathbf{r}'_\parallel,\omega)]d^2r'_\parallel.\end{aligned} \tag{25}$$

By introducing the electric Green function [42]

$$\begin{aligned}\mathbf{G}(\mathbf{r},\omega) = \frac{iq_0}{4\pi}\Bigg\{&\frac{1}{iq_0r}(\mathbf{U} - \hat{\mathbf{r}}\hat{\mathbf{r}}) \\ &- \left[\frac{1}{(iq_0r)^2} - \frac{1}{(iq_0r)^3}\right](\mathbf{U} - 3\hat{\mathbf{r}}\hat{\mathbf{r}})\Bigg\}e^{iq_0r},\end{aligned} \tag{26}$$

Eq. (25) can be written as

$$\mathbf{E}^{(1)}(\mathbf{r};\omega) = 2q_0^2 \left\{ g(r)\hat{\mathbf{n}} \int_{\mathcal{A}} \mathbf{r}'_{\parallel} \cdot \boldsymbol{\mathcal{E}}(\mathbf{r}'_{\parallel};\omega) d^2 r'_{\parallel} - \left[\mathbf{G}(\mathbf{r};\omega) \cdot \int_A \mathbf{r}'_{\parallel} \right] \times [\hat{\mathbf{n}} \times \boldsymbol{\mathcal{E}}(\mathbf{r}'_{\parallel};\omega)] d^2 r'_{\parallel} \right\}, \tag{27}$$

a result which indicates that the first-order contribution (in $r'_{\parallel}/r$) to the diffracted electric field in general is not identical to the field from an ED, $\mathbf{p}(\omega)$, namely [42],

$$\mathbf{E}^{\mathrm{ED}}(\mathbf{r};\omega) = \mu_0 \omega^2 \mathbf{G}(\mathbf{r};\omega) \cdot \mathbf{p}(\omega). \tag{28}$$

Offhand, Eqs. (22) and (27) seem to conflict with the results presented by Bethe and Bouwkamp [9], who calculated the diffracted field from a small circular hole by introducing a fictitious magnetic current density and expanding it in orders of $q_0 a$, where a is the radius of the hole. In the far field they find an ED contribution to the diffracted field in lowest (zeroth) order, and in first order a magnetic dipole contribution is added. Note, however, that the analysis by Bethe and Bouwkamp is fundamentally different from the analysis presented above, as they expand in $q_0 a$, whereas we expand in $r'_{\parallel}/r$.

III. MICROSCOPIC DIFFRACTION THEORY

In classical diffraction from an aperture in an infinitely thin metallic screen of infinite conductivity the central problem is a self-consistent determination of the sheet current density, $\mathbf{J}^S_{\parallel}(\mathbf{r};\omega)$. Once this has been calculated (approximately, in practice) the scattered electromagnetic vector potential, $\mathbf{A}^S(\mathbf{r};\omega)$, can be found everywhere in space outside the screen; see Eq. (10). In turn, the scattered magnetic field is obtained from

$$\mathbf{B}^S(\mathbf{r};\omega) = \nabla \times \mathbf{A}^S(\mathbf{r};\omega), \tag{29}$$

and in the Lorenz gauge [42] the scattered electric field is obtained from

$$\mathbf{E}^S(\mathbf{r};\omega) = i\omega\left(\mathbf{U} + q_0^{-2}\nabla\nabla\right) \cdot \mathbf{A}^S(\mathbf{r};\omega). \tag{30}$$

For a self-consistent approximate calculation and for numerical studies, it is most often *technically* preferable to replace the original problem by its dual problem, at least when the linear extension of the aperture is small compared to the wavelength of the incident field. This is so because the system of differential-integral equations determining the fictitious magnetic current density in the aperture, and thereafter the scattered electric and magnetic fields (see Appendix A), is easier to approximate in a self-consistent manner [9].

In a sense it is obvious that the Bethe-Bouwkamp approach, in which the screen is assumed to be infinitely thin and of infinite conductivity, cannot give us any deep understanding of the indispensable field-matter interaction in the metallic screen. For instance, when the screen becomes sufficiently thin it will tend to behave like a QW (in the z direction), and in the quantum regime the frequency-dependent conductivity cannot be considered as infinite. In the mesoscopic (nano-optical) domain, the screen is not opaque, for certainty. The remarks above do not fail to appreciate that classical diffraction theory has led to many quantitatively excellent results. However, it is also clear that microscopic approaches are needed as the covering theory for the classical studies and in cases where classical diffraction theory is obviously wrong.

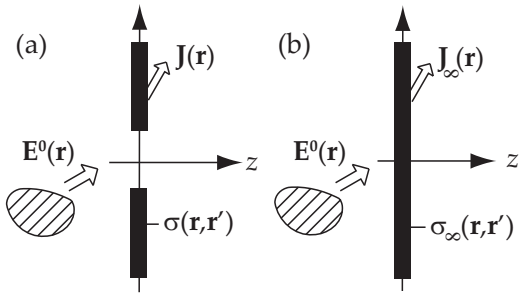

FIG. 2. (a) A system of source charges generates an incident field $\mathbf{E}^0$ which subsequently excites an infinitely extended plane screen with a hole. The screen is in the xy plane and the optical electronic properties of the screen are described by the nonlocal conductivity tensor $\boldsymbol{\sigma}(\mathbf{r},\mathbf{r}')$. The field $\mathbf{E}^0(\mathbf{r})$ induces a self-consistent current density $\mathbf{J}(\mathbf{r})$ in the screen. (b) The same as (a), except that there is no hole in the screen.

A. Microscopic response theory

Let us consider an infinitely extended plane metallic screen of finite thickness and with a hole, and let us assume that the screen is excited by an incident electric field, $\mathbf{E}^0(\mathbf{r};\omega) \equiv \mathbf{E}^0(\mathbf{r})$. The field-matter interaction generates in the screen a microscopic current density, denoted $\mathbf{J}(\mathbf{r},\omega) \equiv \mathbf{J}(\mathbf{r})$ [see Fig. 2(a)]. Assuming that $\mathbf{J}(\mathbf{r})$ has been determined, the total microscopic electric field $\mathbf{E}(\mathbf{r},\omega) \equiv \mathbf{E}(\mathbf{r})$ may be calculated everywhere in space from the integral relation

$$\mathbf{E}(\mathbf{r}) = \mathbf{E}^0(\mathbf{r}) + i\mu_0\omega \int_{-\infty}^{\infty} \mathbf{G}(\mathbf{r},\mathbf{r}') \cdot \mathbf{J}(\mathbf{r}') d^3 r', \tag{31}$$

where $\mathbf{G}(\mathbf{r},\mathbf{r}')$ [$\equiv \mathbf{G}(\mathbf{r},\mathbf{r}';\omega)$] is the standard dyadic Green function relating to vacuum [42,45]. For "observation" points $(\mathbf{r})$ *inside* the screen special care must be shown in the calculation because $\mathbf{G}(\mathbf{r},\mathbf{r}')$ here has an $|\mathbf{r}-\mathbf{r}'|^3$ singularity, stemming from the fact that the Green function contains a nonpropagating part in the metallic domain and its near-field zone [42]. In the framework of conventional microscopic linear response theory, $\mathbf{J}(\mathbf{r})$ is related to $\mathbf{E}(\mathbf{r})$ via the *nonlocal* constitutive relation

$$\mathbf{J}(\mathbf{r}) = \int_{-\infty}^{\infty} \boldsymbol{\sigma}(\mathbf{r},\mathbf{r}') \cdot \mathbf{E}(\mathbf{r}') d^3 r', \tag{32}$$

where $\boldsymbol{\sigma}(\mathbf{r},\mathbf{r}')$ [$\equiv \boldsymbol{\sigma}(\mathbf{r},\mathbf{r}';\omega)$] is the microscopic conductivity tensor, a quantity to be calculated from quantum theory in, say, the random-phase-approximation [46,47]. By substituting Eq. (32) into Eq. (31) one obtains an integral equation for the prevailing field, viz.,

$$\mathbf{E}(\mathbf{r}) = \mathbf{E}^0(\mathbf{r}) + \int_{-\infty}^{\infty} \mathbf{K}(\mathbf{r},\mathbf{r}') \cdot \mathbf{E}(\mathbf{r}') d^3 r', \tag{33}$$

with a frequency-dependent tensorial kernel,

$$\mathbf{K}(\mathbf{r},\mathbf{r}') = i\omega\mu_0 \int_{-\infty}^{\infty} \mathbf{G}(\mathbf{r},\mathbf{r}'') \cdot \boldsymbol{\sigma}(\mathbf{r}'',\mathbf{r}') d^3 r'', \tag{34}$$

including field (**G**) and electronic ($\boldsymbol{\sigma}$) correlation effects at different space points. For observation points inside the screen Eq. (33) provides us with an integral equation for the self-consistent field in the metal. Formally, the solution to Eq. (33) is given by

$$\mathbf{E}(\mathbf{r}) = \int_{-\infty}^{\infty} \boldsymbol{\Gamma}(\mathbf{r},\mathbf{r}') \cdot \mathbf{E}^0(\mathbf{r}') d^3r', \tag{35}$$

where the field-field response tensor (the local field tensor) $\boldsymbol{\Gamma}(\mathbf{r},\mathbf{r}')$ [$\equiv\boldsymbol{\Gamma}(\mathbf{r},\mathbf{r}';\omega)$] satisfies the integral equation

$$\boldsymbol{\Gamma}(\mathbf{r},\mathbf{r}') = \mathbf{U}\delta(\mathbf{r}-\mathbf{r}') + \int_{-\infty}^{\infty} \mathbf{K}(\mathbf{r},\mathbf{r}'') \cdot \boldsymbol{\Gamma}(\mathbf{r}'',\mathbf{r}') d^3r''. \tag{36}$$

Various approximate schemes have been established previously to determine $\boldsymbol{\Gamma}(\mathbf{r},\mathbf{r}')$ from quantum physics in the case where there is no hole in the screen (see Ref. [35], and references herein). Below we realize how the local-field calculation for an infinite screen can be helpful in solving the diffraction problem for a (small) aperture.

Knowledge of $\boldsymbol{\Gamma}(\mathbf{r},\mathbf{r}')$ allows one to establish a *causal* (cau) constitutive relation between the driving (incident) field, $\mathbf{E}^0(\mathbf{r})$, and the induced current density, $\mathbf{J}(\mathbf{r})$, viz.,

$$\mathbf{J}(\mathbf{r}) = \int_{-\infty}^{\infty} \boldsymbol{\sigma}^{\mathrm{cau}}(\mathbf{r},\mathbf{r}') \cdot \mathbf{E}^0(\mathbf{r}') d^3r', \tag{37}$$

where

$$\boldsymbol{\sigma}^{\mathrm{cau}}(\mathbf{r},\mathbf{r}') = \int_{-\infty}^{\infty} \boldsymbol{\sigma}(\mathbf{r},\mathbf{r}'') \cdot \boldsymbol{\Gamma}(\mathbf{r}'',\mathbf{r}') d^3r''. \tag{38}$$

The word *causal* refers to the fact that the relation between $\mathbf{J}$ and $\mathbf{E}^0$ is retarded in the *time domain*. By combining Eq. (31) and Eq. (37), it appears that

$$\mathbf{E}(\mathbf{r}) = \mathbf{E}^0(\mathbf{r}) + i\mu_0\omega \int_{-\infty}^{\infty} \mathbf{G}(\mathbf{r},\mathbf{r}'') \cdot \boldsymbol{\sigma}^{\mathrm{cau}}(\mathbf{r}'',\mathbf{r}') \cdot \mathbf{E}^0(\mathbf{r}') \times d^3r'' d^3r'. \tag{39}$$

In principle, it now appears that the total electric field everywhere in space can be determined by knowledge of the incident field, $\mathbf{E}^0(\mathbf{r})$, and a quantum mechanical (e.g., random-phase approximation) calculation of the microscopic linear conductivity tensor $\boldsymbol{\sigma}(\mathbf{r},\mathbf{r}';\omega)$. The latter quantity depends only on the *optical electronic properties of the metallic screen at* ω, as these appear in the presence of a given aperture.

B. Effective optical aperture

It is intuitively plausible that the diffraction pattern is determined by the field-matter interaction in the vicinity of the aperture, and for a small hole it is convenient to compare the scattering from screens with [Fig. 2(a)] and without [Fig. 2(b)] a hole.

Apart from the disturbance caused by the hole, the two screens are assumed to have identical optical properties, and the incident field is the same in the two cases. To distinguish the two diffraction problems, we add a subscript (∞) to the relevant quantities for the screen without a hole. In the absence of the aperture, Eq. (31), is replaced by

$$\mathbf{E}_\infty(\mathbf{r}) = \mathbf{E}^0(\mathbf{r}) + i\mu_0\omega \int_{-\infty}^{\infty} \mathbf{G}(\mathbf{r},\mathbf{r}') \cdot \mathbf{J}_\infty(\mathbf{r}') d^3r', \tag{40}$$

where

$$\mathbf{J}_\infty(\mathbf{r}) = \int_{-\infty}^{\infty} \boldsymbol{\sigma}_\infty(\mathbf{r},\mathbf{r}') \cdot \mathbf{E}_\infty(\mathbf{r}') d^3r', \tag{41}$$

and we recognize that the vacuum Green function must be the same in Eqs. (31) and (40). By choice the incident field is also the same in the two cases. A procedure analogous to the one described in Sec. III A of course leads to the causal constitutive relation

$$\mathbf{J}_\infty(\mathbf{r}) = \int_{-\infty}^{\infty} \boldsymbol{\sigma}_\infty^{\mathrm{cau}}(\mathbf{r},\mathbf{r}') \cdot \mathbf{E}^0(\mathbf{r}') d^3r' \tag{42}$$

for the aperture-less screen, where $\boldsymbol{\sigma}_\infty^{\mathrm{cau}}(\mathbf{r},\mathbf{r}')$ formally can be obtained from the knowledge of $\boldsymbol{\sigma}_\infty(\mathbf{r},\mathbf{r}')$ and $\mathbf{G}(\mathbf{r},\mathbf{r}')$. By combining Eq. (40) and Eq. (42) one obtains, for the screen without a hole,

$$\mathbf{E}_\infty(\mathbf{r}) = \mathbf{E}^0(\mathbf{r}) + i\mu_0\omega \int_{-\infty}^{\infty} \mathbf{G}(\mathbf{r},\mathbf{r}'') \cdot \boldsymbol{\sigma}_\infty^{\mathrm{cau}}(\mathbf{r}'',\mathbf{r}') \cdot \mathbf{E}^0(\mathbf{r}') \times d^3r'' d^3r'. \tag{43}$$

By subtracting Eq. (43) from Eq. (39) one obtains the important result

$$\mathbf{E}(\mathbf{r};\omega) - \mathbf{E}_\infty(\mathbf{r};\omega) = i\mu_0\omega \int_{-\infty}^{\infty} \mathbf{G}(\mathbf{r},\mathbf{r}'';\omega) \cdot \boldsymbol{\Delta}(\mathbf{r}'',\mathbf{r}';\omega) \cdot \mathbf{E}^0(\mathbf{r}';\omega) d^3r'' d^3r', \tag{44}$$

where

$$\boldsymbol{\Delta}(\mathbf{r},\mathbf{r}';\omega) = \boldsymbol{\sigma}^{\mathrm{cau}}(\mathbf{r},\mathbf{r}';\omega) - \boldsymbol{\sigma}_\infty^{\mathrm{cau}}(\mathbf{r},\mathbf{r}';\omega) \tag{45}$$

in notation where the reference to the frequency has been reinserted. We denote $\boldsymbol{\Delta}(\mathbf{r},\mathbf{r}';\omega)$ the causal effective optical aperture response tensor. Before proceeding with the calculation, let us reflect on the result in Eq. (44). First, we have *not* assumed that the metal-vacuum interfaces are sharp, and in consequence, no jump conditions need to be imposed at the interfaces for either the electromagnetic field or the particle current density at this state of the theory. In a forthcoming paper [36] dealing with a quantum physical calculation of the causal effective aperture response tensor $\boldsymbol{\Delta}(\mathbf{r},\mathbf{r}';\omega)$, we shall discuss the physical approximations needed for a transition from a smooth to a sharp metal-vacuum interface model. Second, $\boldsymbol{\Delta}(\mathbf{r},\mathbf{r}';\omega)$ is nonvanishing only in and close to the aperture (see Fig. 3).

The words *close to* here refer to the so-called spatial correlation length, d_c, a concept which in a qualitative sense determines how far the spatial points $\mathbf{r}$ and $\mathbf{r}'$ need to be separated before the microscopic conductivity tensor $\boldsymbol{\sigma}^{\mathrm{cau}}(\mathbf{r},\mathbf{r}';\omega)$ [or $\boldsymbol{\sigma}_\infty^{\mathrm{cau}}(\mathbf{r},\mathbf{r}';\omega)$] vanishes. At distances from the hole larger than $\sim d_c$ the response tensor $\boldsymbol{\sigma}^{\mathrm{cau}}(\mathbf{r},\mathbf{r}';\omega)$ becomes identical to $\boldsymbol{\sigma}_\infty^{\mathrm{cau}}(\mathbf{r},\mathbf{r}';\omega)$. Third, the electromagnetic diffraction problem has been transferred to its roots, viz., a (quantum mechanical) calculation of the electromagnetic properties of the screen with a given aperture. Fourth, for small holes it appears advantageously from an experimental point of view to compare (subtract) the diffraction from screens with and without a hole both excited by the same incident field (see also Sec. IV). Fifth, there is no need to assume that the screen is

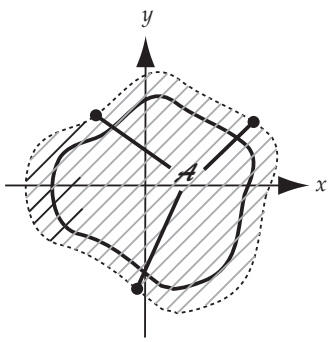

FIG. 3. The effective optical aperture in the plane of the screen—henceforth denoted $\mathcal{A}$—is the area defined by the region where $\boldsymbol{\sigma}^{\mathrm{cau}} - \boldsymbol{\sigma}_{\infty}^{\mathrm{cau}}$ is nonvanishing. Note that $\mathcal{A}$ is lager than the geometrical aperture indicated by the thick solid line.

opaque. The source region for the difference field $(\mathbf{E} - \mathbf{E}_{\infty})$ we call the *effective optical aperture* (cf. Fig. 3).

C. Electric-dipole absorber sheet

Let us now assume that the thickness of the screen is so small that the variation of the incident field across the screen (in the z direction) is negligible. By dividing the given position coordinate [$\mathbf{r}$ (or $\mathbf{r}'$)] into its components parallel ($\mathbf{r}_{\parallel}$) and perpendicular ($\mathbf{r}_{\perp} = z\hat{\mathbf{z}}$) to the plane of the screen, i.e., $\mathbf{r} = \mathbf{r}_{\parallel} + z\hat{\mathbf{z}}$, the current density, $\mathbf{J}(\mathbf{r}) \equiv \mathbf{J}(\mathbf{r}_{\parallel}, z)$, in Eq. (37) takes the approximate form

$$\mathbf{J}(\mathbf{r}_{\parallel}, z) = \int_{-\infty}^{\infty} \left[\int_{\mathrm{QW}} \boldsymbol{\sigma}^{\mathrm{cau}}(\mathbf{r}_{\parallel}, \mathbf{r}'_{\parallel}, z, z') dz' \right] \cdot \mathbf{E}^{0}(\mathbf{r}'_{\parallel}, 0) d^{2}r'_{\parallel}, \tag{46}$$

where $\mathbf{E}^{0}(\mathbf{r}'_{\parallel}, z') = \mathbf{E}^{0}(\mathbf{r}'_{\parallel}, 0)$ for all z' coordinates inside the screen. We have added the subscript QW to the integral sign of the z' integration to indicate that a sufficiently thin screen becomes a QW from a microscopic point of view. In what follows a thin current sheet is therefore sometimes referred to as a QW (sheet). Since the screen obviously must be at least one monolayer thick, the approximation in Eq. (46) requires that the characteristic wavelength (variation length) of the incident field must be larger than that of x rays. If needed, one may go beyond the approximation in Eq. (46) by making a Taylor series expansion of $\mathbf{E}^{0}(\mathbf{r}'_{\parallel}, z')$ in z' around the origo. In the lowest order approximation [Eq. (46)] the QW sheet behaves electromagnetically as an ED absorber [34].

D. Electric-dipole radiator sheet

When the screen is sufficiently thin it also behaves in lowest order as an ED radiator sheet [34]. In order to quantify this we return to Eq. (39), written as

$$\mathbf{E}(\mathbf{r}_{\parallel}, z) - \mathbf{E}^{0}(\mathbf{r}_{\parallel}, z) = i\mu_{0}\omega \int_{-\infty}^{\infty} \mathbf{G}(\mathbf{r}_{\parallel}, \mathbf{r}'_{\parallel}, z, z') \cdot \mathbf{J}(\mathbf{r}'_{\parallel}, z') dz' d^{2}r'_{\parallel}, \tag{47}$$

where $\mathbf{G}(\mathbf{r}_{\parallel}, \mathbf{r}'_{\parallel}, z, z')$ ends up being the Green's function in disk contraction [48–50]. Its explicit form in the mixed (angular spectrum) representation is given in Sec. III G. At lowest order the variation of the Green function across the current sheet is neglected, that is, $\mathbf{G}(\mathbf{r}_{\parallel}, \mathbf{r}'_{\parallel}, z, z') = \mathbf{G}(\mathbf{r}_{\parallel}, \mathbf{r}'_{\parallel}, z, 0)$ in Eq. (47). Hence

$$\mathbf{E}(\mathbf{r}_{\parallel}, z) - \mathbf{E}^{0}(\mathbf{r}_{\parallel}, z) = i\mu_{0}\omega \int_{-\infty}^{\infty} \mathbf{G}(\mathbf{r}_{\parallel}, \mathbf{r}'_{\parallel}, z, 0) \cdot \mathbf{J}^{S}(\mathbf{r}'_{\parallel}) d^{2}r'_{\parallel}, \tag{48}$$

where

$$\mathbf{J}^{S}(\mathbf{r}_{\parallel}) = \int_{\mathrm{QW}} \mathbf{J}(\mathbf{r}_{\parallel}, z) dz. \tag{49}$$

In the moment expansion of a localized current distribution [42], here in one dimension, the sheet current density is, at lowest (zero) order, given by

$$\mathbf{J}^{(0)}(\mathbf{r}_{\parallel}, z) = \mathbf{J}^{S}(\mathbf{r}_{\parallel}) \delta(z). \tag{50}$$

Inserting this form into Eq. (47) one regains Eq. (48) of course. The result in Eq. (48) may, if desired, be obtained starting from Eq. (10) [42].

E. ED-ED sheet. Aperture response tensor

In the consistent approximation where the screen behaves both as an ED absorber and as an ED radiator (we call such a sheet an ED-ED sheet [34]), a combination of Eq. (46) and Eq. (49) shows that

$$\mathbf{J}^{S}(\mathbf{r}_{\parallel}) = \int_{-\infty}^{\infty} \mathbf{S}(\mathbf{r}_{\parallel}, \mathbf{r}'_{\parallel}) \cdot \mathbf{E}^{0}(\mathbf{r}'_{\parallel}) d^{2}r'_{\parallel}, \tag{51}$$

where the quantity

$$\mathbf{S}(\mathbf{r}_{\parallel}, \mathbf{r}'_{\parallel}) = \int_{\mathrm{QW}} \boldsymbol{\sigma}^{\mathrm{cau}}(\mathbf{r}_{\parallel}, \mathbf{r}'_{\parallel}, z, z') dz' dz \tag{52}$$

may be called the causal surface (or ED-ED sheet) conductivity response tensor. In Eq. (51) we have, for brevity, written $\mathbf{E}^{0}(\mathbf{r}'_{\parallel}, 0) = \mathbf{E}^{0}(\mathbf{r}'_{\parallel})$. A result analogous to the one given by Eqs. (51) and (52) may be derived for the screen without an aperture, of course. Thus,

$$\mathbf{J}_{\infty}^{S}(\mathbf{r}_{\parallel}) = \int_{-\infty}^{\infty} \mathbf{S}_{\infty}(\mathbf{r}_{\parallel}, \mathbf{r}'_{\parallel}) \cdot \mathbf{E}^{0}(\mathbf{r}'_{\parallel}) d^{2}r'_{\parallel}, \tag{53}$$

with

$$\mathbf{S}_{\infty}(\mathbf{r}_{\parallel}, \mathbf{r}'_{\parallel}) = \int_{\mathrm{QW}} \boldsymbol{\sigma}_{\infty}^{\mathrm{cau}}(\mathbf{r}_{\parallel}, \mathbf{r}'_{\parallel}, z, z') dz' dz. \tag{54}$$

Let us now return to the central result in Eq. (44), and herein make the ED-ED sheet approximation. This gives the result

$$\mathbf{E}(\mathbf{r}; \omega) - \mathbf{E}_{\infty}(\mathbf{r}; \omega) = i\mu_{0}\omega \int_{\mathcal{A}} \mathbf{G}(\mathbf{r}_{\parallel}, \mathbf{r}'_{\parallel}, z; \omega) \cdot \boldsymbol{\Delta}(\mathbf{r}'_{\parallel}, \mathbf{r}''_{\parallel}; \omega) \cdot \mathbf{E}^{0}(\mathbf{r}''_{\parallel}; \omega) d^{2}r''_{\parallel} d^{2}r'_{\parallel}, \tag{55}$$

where

$$\Delta(\mathbf{r}_{\parallel}, \mathbf{r}'_{\parallel}; \omega) = \mathbf{S}(\mathbf{r}_{\parallel}, \mathbf{r}'_{\parallel}; \omega) - \mathbf{S}_{\infty}(\mathbf{r}_{\parallel}, \mathbf{r}'_{\parallel}; \omega). \tag{56}$$

In Eq. (55) $\mathbf{G}(\mathbf{r}_{\parallel}, \mathbf{r}'_{\parallel}, z; \omega) \equiv \mathbf{G}(\mathbf{r}_{\parallel}, \mathbf{r}'_{\parallel}, z, z' = 0; \omega)$ and $\mathbf{E}^{0}(\mathbf{r}''_{\parallel}; \omega) \equiv \mathbf{E}^{0}(\mathbf{r}''_{\parallel}, z'' = 0; \omega)$. The quantity $\boldsymbol{\Delta}(\mathbf{r}_{\parallel}, \mathbf{r}'_{\parallel}; \omega)$ we call the *ED-ED aperture response tensor* because it is nonvanishing only in the *effective aperture region* ($\mathcal{A}$), a plane area here (cf. Fig. 3). To emphasize this we have written

$\int_{\mathcal{A}}(\dots)$ instead of $\int_{-\infty}^{\infty}(\dots)$ above. For the purposes of this article Eq. (55) is a central result, showing that the entire diffraction problem (for a thin screen) essentially can be turned into (reduced to) a quantum mechanical calculation of the spatially nonlocal ED-ED aperture response tensor, $\mathbf{\Delta}(\mathbf{r}_\parallel,\mathbf{r}'_\parallel;\omega)$. A general quantum mechanical calculation of the aperture response tensor is a comprehensive task, which is outside the scope of the present work. However, in Sec. V we present a calculation for perhaps the simplest case of all, namely, a one-level QW screen.

F. Scattering from small apertures

It is of particular importance, e.g., in nano-optics and quantum optics, to study diffraction from small holes. By small we refer to a situation where the ratio between the correlation length (d_c) and the characteristic length parameter (Λ) of the electromagnetic field is so low that $\mathbf{E}^0$ and $\mathbf{G}$ can be expanded in a Taylor series in $\mathbf{r}''_\parallel$ and $\mathbf{r}'_\parallel$ around the origo. If the aperture is located in the far field of the incident field, the wavelength (λ_0) of $\mathbf{E}^0$ is this field's Λ. It turns out that the Green function may involve evanescent modes. These mode's length parameter can be much smaller than λ_0 (see Sec. III G). At lowest order, one neglects the variation of $\mathbf{E}^0$ and $\mathbf{G}$ across the aperture. This approximation one may denote an ED-ED approximation (here with respect to the coordinates parallel to the plane of the screen).

Let us introduce the difference field,

$$\mathbf{E}^{\mathcal{A}}(\mathbf{r};\omega)=\mathbf{E}(\mathbf{r};\omega)-\mathbf{E}_\infty(\mathbf{r};\omega), \tag{57}$$

and call this field the *aperture field*. From Eq. (55) we find that this field in the ED-ED approximation is given as

$$\mathbf{E}^{\mathcal{A}}(\mathbf{r};\omega)=i\mu_0\omega\mathbf{G}(\mathbf{r}_\parallel,z;\omega)\cdot\mathbf{\Delta}(\omega)\cdot\mathbf{E}^0(\mathbf{0},\omega), \tag{58}$$

where

$$\mathbf{\Delta}(\omega)=\int_{\mathcal{A}}\mathbf{\Delta}(\mathbf{r}_\parallel,\mathbf{r}'_\parallel;\omega)d^2r'_\parallel d^2r_\parallel. \tag{59}$$

In Eq. (58), the natural notational abbreviations $\mathbf{E}^0(\mathbf{r}_\parallel=\mathbf{0},z=0;\omega)\equiv\mathbf{E}^0(\mathbf{0};\omega)$ and $\mathbf{G}(\mathbf{r}_\parallel,\mathbf{r}'_\parallel=\mathbf{0},z,z'=0;\omega)\equiv\mathbf{G}(\mathbf{r}_\parallel,z;\omega)$ are used. A comparison of Eq. (28) and Eq. (58) shows that the field from the effective aperture in the ED-ED limit is identical to the field of an ED with a dipole moment given by

$$\mathbf{p}(\omega)=\frac{i}{\omega}\mathbf{\Delta}(\omega)\cdot\mathbf{E}^0(\mathbf{0};\omega) \tag{60}$$

and placed at the center of the aperture ($\mathbf{r}=0$), as indicated. The frequency-dependent ED polarizability tensor, $(i/\omega)\mathbf{\Delta}(\omega)$, thus is obtained from a quantum mechanical calculation of $\mathbf{\Delta}(\omega)$ in our microscopic theory. Note that we have not assumed that the small hole has a specific form. However, it is obvious that the mutual relations between the various complex tensor elements of $\mathbf{\Delta}(\omega)$ depend on the aperture's geometrical form.

As noted in Sec. II D, in the Bethe-Bouwkamp theory for a circular hole of radius a in an isotropic infinitely thin screen of infinite conductivity (σ) the aperture far field is, at lowest order of q_0a, that of an ED. At the next order a magnetic-dipole field is added [9]. It is of overriding importance to understand that the Bethe-Bouwkamp theory to second order basically has only one parameter, namely, the radius of the hole, a, because the assumption $\sigma\to\infty$ is made. In general, one would certainly not expect this parameter to describe the physics of diffraction correctly (e.g., at all frequencies; see also Sec. IV). To make a connection with the Bethe-Bouwkamp approach, let us assume that our 2D system (screen plus hole) exhibits infinitesimal rotational symmetry around the z axis *and* reflection symmetry with respect to an arbitrary plane containing the z axis (say, the plane $x=0$). In this case, it appears that

$$\mathbf{\Delta}(\omega)=(\mathbf{U}-\hat{\mathbf{z}}\hat{\mathbf{z}})\Delta_\parallel(\omega)+\hat{\mathbf{z}}\hat{\mathbf{z}}\Delta_\perp(\omega), \tag{61}$$

and one is left with at least two frequency-dependent parameters, $\Delta_\parallel(\omega)$ and $\Delta_\perp(\omega)$.

G. Jump conditions for the aperture field

We now return to Eq. (55). Due to the fact that here we have reduced the electrodynamics in the z direction to that of a δ function sheet, one cannot expect to uphold the continuity of the microscopic aperture field across the effective aperture (Fig. 3). To investigate this point let us introduce the aperture surface current density,

$$\mathbf{J}^{\mathcal{A}}(\mathbf{r}_\parallel)=\int_{\mathcal{A}}\mathbf{\Delta}(\mathbf{r}_\parallel,\mathbf{r}'_\parallel)\cdot\mathbf{E}^0(\mathbf{r}'_\parallel)d^2r'_\parallel. \tag{62}$$

In view of the fact that the vacuum Green function necessarily has infinitesimal translation invariance along any direction parallel to the sheet plane, i.e.,

$$\mathbf{G}(\mathbf{r}_\parallel,\mathbf{r}'_\parallel,z)=\mathbf{G}(\mathbf{r}_\parallel-\mathbf{r}'_\parallel,z), \tag{63}$$

and because the integration(s) over $\mathcal{A}$ can be extended to infinity since $\mathbf{\Delta}(\mathbf{r}_\parallel,\mathbf{r}'_\parallel)$ vanishes outside the effective aperture region, the convolution theorem leads to the following algebraic relation:

$$\mathbf{E}^{\mathcal{A}}(\mathbf{q}_\parallel;z)=i\mu_0\omega\mathbf{G}(\mathbf{q}_\parallel,z)\cdot\mathbf{J}^{\mathcal{A}}(\mathbf{q}_\parallel). \tag{64}$$

Physically, $\mathbf{q}_\parallel$ is the wave vector of the various field quantities parallel to the plane of the sheet. In the above, so-called mixed representation [42], the Green function must be described in disk contraction [48–50] and thus is given by the dyadic form

$$\begin{aligned}\mathbf{G}(\mathbf{q}_\parallel,z)=q_0^{-2}\delta(z)\hat{\mathbf{z}}\hat{\mathbf{z}}+\frac{i}{2\kappa_\perp q_0^2}e^{i\kappa_\perp|z|}\big[q_0^2\mathbf{U}-\mathbf{q}_\parallel\mathbf{q}_\parallel\\ -\kappa_\perp^2\hat{\mathbf{z}}\hat{\mathbf{z}}-(\mathbf{q}_\parallel\hat{\mathbf{z}}+\hat{\mathbf{z}}\mathbf{q}_\parallel)\kappa_\perp\mathrm{sgn}(z)\big],\end{aligned} \tag{65}$$

with

$$\kappa_\perp=\begin{cases}\left(q_0^2-q_\parallel^2\right)^{1/2} & \text{for}\quad q_\parallel<q_0\ \text{(propagating modes)},\\ i\left(q_\parallel^2-q_0^2\right)^{1/2} & \text{for}\quad q_\parallel>q_0\ \text{(evanescent modes)}.\end{cases} \tag{66}$$

The first term in Eq. (65) relates to the self-field inside the screen. For a δ function sheet, this term must be neglected in advance, of course.

The jump of the aperture field across the $z=0$ plane (from $z=0^-$ to $z=0^+$) is readily obtain from Eqs. (64) and (65). Hence,

$$\mathrm{Jump}[i\mu_0\omega\mathbf{G}(\mathbf{q}_\parallel,z)\cdot\mathbf{J}^{\mathcal{A}}(\mathbf{q}_\parallel)]=\frac{1}{\varepsilon_0\omega}(\mathbf{q}_\parallel\hat{\mathbf{z}}+\hat{\mathbf{z}}\mathbf{q}_\parallel)\cdot\mathbf{J}^{\mathcal{A}}(\mathbf{q}_\parallel). \tag{67}$$

By utilizing Fourier transformation and by dividing the aperture current density into its components parallel ($\mathbf{J}_\parallel^{\mathcal{A}}$) and perpendicular ($J_\perp^{\mathcal{A}} = \hat{\mathbf{z}} \cdot \mathbf{J}^{\mathcal{A}}$) to the QW plane, the following jumps for the components of the aperture field parallel and perpendicular to $z = 0$ emerge:

$$\mathbf{E}_\parallel^{\mathcal{A}}(\mathbf{r}_\parallel, 0^+) - \mathbf{E}_\parallel^{\mathcal{A}}(\mathbf{r}_\parallel, 0^-) = \frac{1}{i\varepsilon_0\omega} \nabla_\parallel J_\perp^{\mathcal{A}}(\mathbf{r}_\parallel), \tag{68}$$

$$E_\perp^{\mathcal{A}}(\mathbf{r}_\parallel, 0^+) - E_\perp^{\mathcal{A}}(\mathbf{r}_\parallel, 0^-) = \frac{1}{i\varepsilon_0\omega} \nabla_\parallel \cdot \mathbf{J}_\parallel^{\mathcal{A}}(\mathbf{r}_\parallel). \tag{69}$$

In the Bethe-Bouwkamp approach, as well as in all other classical theories (to the best of our knowledge), it is assumed that $J_\perp^{\mathcal{A}} = 0$, as mentioned in Sec. II B. In Appendix B, we study the boundary conditions in the physically important case where $J_\perp \neq 0$.

IV. REMARKS ON THE INTERPLAY BETWEEN THEORY AND EXPERIMENT

In 1995, Obermüller and Karrai published an experimental paper on the far-field angular intensity distribution of light ($\lambda_0 = 633$ nm) diffracted from subwavelength circular apertures (radius a) located at the apex of Al-coated optical fiber tips [51]. A primary goal was to propose a method which allows one to determine the effective optical size of subwavelength holes. In the small-radius limit ($q_0 a \ll 1$) the authors compared their data to the Bethe theory, in which the far-field radiation is identical to the field obtained by a combination of an in-plane magnetic dipole (moment $\mathbf{m}$) oriented antiparallel to the magnetic field $\mathbf{H}_0$ (the field on the $z = 0^-$ side of the screen if there is no hole) and an ED (moment $\mathbf{p}$) directed perpendicular to the screen and proportional to the zeroth-order electric field $\mathbf{E}^0 = \mathbf{E}_\perp^0$ at $z = 0^-$ (see below).

Obermüller and Karrai concluded that Bethe's theory failed to describe their data. However, to the authors' surprise, they found that the data could be fitted perfectly for a choice of $\mathbf{m}$ and $\mathbf{p}$ proportional to that of Bethe, but with $\mathbf{p}$ lying in the aperture plane in the direction parallel to $\mathbf{E}_{\text{fiber}}^0$, the field in the fiber in the front of the aperture, and with $\mathbf{m}$ directed parallel to $\mathbf{H}_{\text{fiber}}^0$. Thus, in the Gaussian units used by Bethe,

$$\mathbf{p} = \frac{a^3}{3\pi} \alpha \mathbf{E}_{\text{fiber}}^0 \tag{70}$$

and

$$\mathbf{m} = \frac{2a^3}{3\pi} (\mu_0 c) \alpha \mathbf{H}_{\text{fiber}}^0, \tag{71}$$

where α is an *unknown proportionality factor*. Since the boundary condition of the field plays a crucial role for the diffraction problem, it is not surprising that there is a discrepancy between the flat-screen model and the coated-fiber-tip data, as emphasized by Obermüller and Karrai. To first order in $q_0 a$, the Bethe-Bouwkamp theory represents the far field by a superposition of the fields from the dipoles,

$$\mathbf{p} = \frac{a^3}{3\pi} \mathbf{E}^0, \quad \mathbf{m} = -\frac{2a^3}{3\pi} \mathbf{H}^0, \tag{72}$$

$\mathbf{E}^0 = \mathbf{E}_\perp^0$ and $\mathbf{H}^0 = \mathbf{H}_\parallel^0$ being the fields (at the origo) if there is no hole in the screen.

Putting aside the question of the orientation of the dipoles, it appears from Eq. (72), as also noted in Sec. III F, that the Bethe-Bouwkamp theory has only one polarizability parameter, viz., the hole radius a (to the third power). From a physical point of view, this gives their approach a limited scope. The electric and magnetic polarizabilities (at least) must be frequency dependent, since diffraction in the small hole originates in the electrodynamic field-matter interaction. In the Bethe-Bouwkamp model, where the conductivity is assumed to be infinite, this interaction is blocked. In Eqs. (70) and (71), there is also one common polarizability parameter, namely, $a^3\alpha$. In principle, α may depend on the electromagnetic frequency, $\alpha = \alpha(\omega)$, but in Ref. [51] this possibility is not examined since all angular distributions refer to a single frequency. Some experiments in the literature [23,52–56] do study the frequency dependence of small-hole polarizabilities. In the paper by Adam *et al.* [55] the frequency dependence of the near-field diffraction is measured in the terahertz region. The data obtained are in agreement with the Bouwkamp theory, as one perhaps might expect at these long wavelengths. A comparison of our theory to experiments dealing with plasmon effects in small-hole diffraction [23,52–54,56] will require that the pole structure of the aperture response tensor be analyzed. We address this issue in a forthcoming paper [36]. From a theoretical point of view we consider frequency-resolved experiments of crucial importance. In our microscopic diffraction theory the aperture response tensor has a least two frequency-dependent parameters, $\Delta_\parallel(\omega)$ and $\Delta_\perp(\omega)$ [see Eq. (61)]. These parameters are not intrinsically independent of course. In the ED-ED limit the effective aperture radiates in our theory like an ED with anisotropic polarizabilty, i.e.,

$$\mathbf{p}(\omega) = \frac{i}{\omega} (\Delta_\parallel(\omega) \mathbf{E}_\parallel^0 + \Delta_\perp(\omega) \mathbf{E}_\perp^0). \tag{73}$$

Curiously, we find that contributions from EDs oriented both perpendicular (theory of Bethe) and parallel (experiments by Obermüller and Karrai) are needed to account for the diffraction from small circular holes in isotropic screens [cf. the remarks preceding Eq. (61)].

In view of the fact that there exists a variety of theoretical models dealing with optical diffraction from small holes, we consider it important to obtain more experimental information. In particular, it would be stimulating to carry out measurements on a metallic (or semiconducting) QW screen with a small (ED-ED) hole. Since a QW (with a few bound energy levels) will be quite transparent, and the diffraction from the hole very small, it appears favorable in our view to carry out some kind of interference experiment on QWs without (shifted π in phase) and with a hole.

V. APERTURE RESPONSE TENSOR FOR A SINGLE-LEVEL QUANTUM-WELL SCREEN WITH DIAMAGNETIC ELECTRON DYNAMICS

To accomplish a quantum mechanical calculation of the aperture response tensor it is necessary to restrict the analysis to simple situations (systems). In this section we carry out

a calculation for perhaps the simplest case of all, namely, a one-level metallic (or semiconducting) QW screen subjected to optical radiation with frequencies in the mid- and far-infrared regions. The chosen example offers additional physical insight into the various processes hidden in the microscopic diffraction theory advanced in Sec. III.

In the frequency range mentioned above, the microscopic conductivity of a metallic (or semiconducting) mesoscopic medium usually is well described retaining only the diamagnetic part of $\boldsymbol{\sigma}(\mathbf{r},\mathbf{r}';\omega)$ (see Ref. [57], and references therein), that is,

$$\boldsymbol{\sigma}(\mathbf{r},\mathbf{r}';\omega) = \Sigma(\mathbf{r};\omega)\delta(\mathbf{r}-\mathbf{r}')\mathbf{U}, \tag{74}$$

with

$$\Sigma(\mathbf{r},\omega) = \frac{ie^2}{m(\omega+i/\tau)}n^0(\mathbf{r}), \tag{75}$$

where e and m are the electron charge and mass, and τ is the (phenomenological) electron momentum relaxation time. The quantity $n^0(\mathbf{r})$ is the field-unperturbed electron density at space point $\mathbf{r}$. In the random-phase approximation $n^0(\mathbf{r})$ in thermal equilibrium is given by [47,57]

$$n^0(\mathbf{r}) = 2\sum_{\mathbf{k}} f_{\mathbf{k}}|\psi_{\mathbf{k}}(\mathbf{r})|^2, \tag{76}$$

where $\psi_{\mathbf{k}}(\mathbf{r})$ is the electron Schrödinger wave function of the single-particle state $\mathbf{k}$, and $f_{\mathbf{k}} \equiv f(\varepsilon_{\mathbf{k}})$ is the Fermi-Dirac distribution factor belonging to the energy $\varepsilon_{\mathbf{k}}$. The summation in Eq. (76) runs over all $\mathbf{k}$ states and the factor of 2 stems from the assumed spin degeneracy. Although the overall diamagnetic conductivity is spatially local and isotropic, the individual electronic transitions contributing to this conductivity are nonlocal and anisotropic, as they must be [42]. With $\boldsymbol{\sigma}$ given by Eq. (74), the causal conductivity tensor takes the form

$$\boldsymbol{\sigma}^{\text{cau}}(\mathbf{r},\mathbf{r}';\omega) = \Sigma(\mathbf{r};\omega)\boldsymbol{\Gamma}(\mathbf{r},\mathbf{r}';\omega). \tag{77}$$

The nonlocality and anisotropy of $\boldsymbol{\sigma}^{\text{cau}}$ thus are associated solely with the field-field response tensor. This tensor is determined from Eq. (36), with the kernel $\mathbf{K}(\mathbf{r},\mathbf{r}';\omega) = i\mu_0\omega\mathbf{G}(\mathbf{r},\mathbf{r}';\omega)\Sigma(\mathbf{r}';\omega)$. Since it is unlikely that an exact analytical solution can be found, we rely on an iterative solution, namely,

$$\boldsymbol{\Gamma}(\mathbf{r},\mathbf{r}') = \mathbf{U}\delta(\mathbf{r}-\mathbf{r}') + i\mu_0\omega\Sigma(\mathbf{r}')\mathbf{G}(\mathbf{r},\mathbf{r}') + (i\mu_0\omega)^2 \times \int_{-\infty}^{\infty}\Sigma(\mathbf{r}'')\mathbf{G}(\mathbf{r},\mathbf{r}'')\cdot\mathbf{G}(\mathbf{r}'',\mathbf{r}')\Sigma(\mathbf{r}')d^3r'' + \ldots. \tag{78}$$

In the *first Born approximation*, where only the two first terms on the right side of Eq. (78) are retained, the causal conductivity tensor is given by

$$\boldsymbol{\sigma}^{\text{cau}}(\mathbf{r},\mathbf{r}';\omega) = \boldsymbol{\sigma}(\mathbf{r},\mathbf{r}';\omega) + i\mu_0\omega\Sigma(\mathbf{r};\omega)\mathbf{G}(\mathbf{r},\mathbf{r}';\omega)\Sigma(\mathbf{r}';\omega). \tag{79}$$

The result in Eq. (79) exemplifies the important fact that the correlation effects in the causal conductivity tensor between the space points $\mathbf{r}$ and $\mathbf{r}'$ are of both electronic and electromagnetic origin. Thus, $\boldsymbol{\sigma}(\mathbf{r},\mathbf{r}';\omega)$ describes the electronic δ function correlation, and $\Sigma(\mathbf{r};\omega)\mathbf{G}(\mathbf{r},\mathbf{r}';\omega)\Sigma(\mathbf{r}';\omega)$ the direct (lowest order) electromagnetic correlation. This is illustrated schematically in Fig. 4.

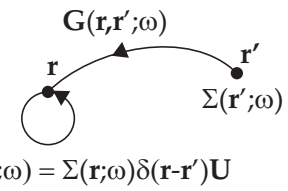

FIG. 4. Electronic δ function and (lowest order) direct electromagnetic correlation effects in the causal conductivity tensor, $\boldsymbol{\sigma}^{\text{cau}}(\mathbf{r},\mathbf{r}';\omega)$.

In a QW context the thinnest possible screen is one containing only one bound QW level. In such a single-level (SL) QW the bound electron motion is confined to a plane (here $z = 0$), essentially. In the diamagnetic case this means that

$$\Sigma(\mathbf{r};\omega) = \Sigma^{\text{SL}}(\mathbf{r}_\parallel;\omega)\delta(z). \tag{80}$$

Within the first Born approximation the causal surface conductivity tensor for a single-level QW, $\mathbf{S}^{\text{SL}}(\mathbf{r}_\parallel,\mathbf{r}'_\parallel;\omega)$, is obtained by combining Eqs. (52), (74), (79), and (80). Hence, one gets

$$\mathbf{S}^{\text{SL}}(\mathbf{r}_\parallel,\mathbf{r}'_\parallel;\omega) = \mathbf{U}\Sigma^{\text{SL}}(\mathbf{r}_\parallel;\omega)\delta(\mathbf{r}_\parallel-\mathbf{r}'_\parallel) + i\mu_0\omega \times \Sigma^{\text{SL}}(\mathbf{r}_\parallel;\omega)\mathbf{G}(\mathbf{r}_\parallel,\mathbf{r}'_\parallel;\omega)\Sigma^{\text{SL}}(\mathbf{r}'_\parallel;\omega), \tag{81}$$

with the abbreviation $\mathbf{G}(\mathbf{r}_\parallel,\mathbf{r}'_\parallel,z=0,z'=0;\omega) = \mathbf{G}(\mathbf{r}_\parallel,\mathbf{r}'_\parallel;\omega)$.

To determine the ED-ED aperture response tensor

$$\begin{aligned}\boldsymbol{\Delta}(\mathbf{r}_\parallel,\mathbf{r}'_\parallel;\omega) &= \mathbf{U}\left[\Sigma^{\text{SL}}(\mathbf{r}_\parallel;\omega) - \Sigma^{\text{SL}}_\infty(\mathbf{r}_\parallel;\omega)\right]\delta(\mathbf{r}_\parallel-\mathbf{r}'_\parallel) + \ldots \\ &= \frac{ie^2\mathbf{U}}{m(\omega+i/\tau)}\left[n^0(\mathbf{r}_\parallel) - n^0_\infty(\mathbf{r}_\parallel)\right]\delta(\mathbf{r}_\parallel-\mathbf{r}'_\parallel) + \ldots,\end{aligned} \tag{82}$$

we need to calculate the 2D electron density,

$$n^0(\mathbf{r}_\parallel) = 2\sum_{\mathbf{k}_\parallel} f_{\mathbf{k}_\parallel}|\psi^T(\mathbf{r}_\parallel;\mathbf{k}_\parallel)|^2, \tag{83}$$

and an analogous expression for $n^0_\infty(\mathbf{r}_\parallel)$ in which $\psi^T(\mathbf{r}_\parallel;\mathbf{k}_\parallel)$ is replaced by the plane-wave state $\psi^\infty_{\mathbf{k}_\parallel}(\mathbf{r}_\parallel)$. By means of a recently established 2D extinction theorem for electrons the non-plane-wave function $\psi^T(\mathbf{r}_\parallel;\mathbf{k}_\parallel)$ can be related to $\psi^\infty_{\mathbf{k}_\parallel}(\mathbf{r}_\parallel)$ [36]. In its general form the extinction theorem allows one to handle the physics in the selvedge region separating the bulk potential of the screen from the hole potential. In the framework of the so-called infinite-barrier model [58] one obtains the integral equation for $\psi^T(\mathbf{r}_\parallel;\mathbf{k}_\parallel)$ [T for total (wave function)]

$$\psi^T(\mathbf{r}_\parallel;\mathbf{k}_\parallel) = \psi^\infty_{\mathbf{k}_\parallel}(\mathbf{r}_\parallel) + \psi^S(\mathbf{r}_\parallel;\mathbf{k}_\parallel) = \psi^\infty_{\mathbf{k}_\parallel}(\mathbf{r}_\parallel) - \oint_{C_0}\mathcal{G}(k_\parallel|\mathbf{r}_\parallel-\mathbf{r}'_\parallel|)\hat{\mathbf{n}}_0(\mathbf{r}'_\parallel)\cdot\nabla'_\parallel\psi^T(\mathbf{r}_\parallel;\mathbf{k}_\parallel)dr'_\parallel, \tag{84}$$

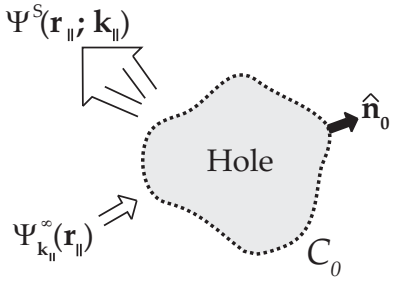

FIG. 5. Scattering of the electron wave function from the hole in the QW screen.

where the one-dimensional integral runs over the contour (C_0) of the hole. The quantity $\hat{\mathbf{n}}_0$ is an outward directed normal to C_0. The line integral in Eq. (84) describes the scattered part, $\psi^S(\mathbf{r}_\parallel;\mathbf{k}_\parallel)$, of the total wave function $\psi^T(\mathbf{r}_\parallel;\mathbf{k}_\parallel)$. The scattered wave function from the various space points ($\mathbf{r}'_\parallel$) on the contour propagates back into the screen in a manner given by the outgoing 2D electron scalar propagator,

$$\mathcal{G}(k_\parallel \mathbf{R}_\parallel) = \frac{i}{4} H_0^{(1)}(k_\parallel R_\parallel), \tag{85}$$

$H_0^{(1)}$ being the zeroth-order Hankel function of the first kind. A schematic of the 2D scattering geometry is shown in Fig. 5.

The integral equation in Eq. (84) may be solved by iteration (Born series approach) or numerically.

When combined with Eqs. (82) and (83) the result in Eq. (84) forms the basis for understanding the *effective optical aperture* concept (Fig. 3), in particular, the extension of $\mathcal{A}$ outside the hole, here within the framework of the infinite-barrier model. Neglecting local-field effects [$\mathbf{\Gamma}(\mathbf{r},\mathbf{r}') = \mathbf{U}\delta(\mathbf{r}-\mathbf{r}')$], $\boldsymbol{\sigma}^{\rm cau}(\mathbf{r},\mathbf{r}';\omega) = \boldsymbol{\sigma}(\mathbf{r},\mathbf{r}';\omega)$, and in this approximation, the extension of $\mathcal{A}$ into the screen is given by $n^0(\mathbf{r}_\parallel) - n^0_\infty(\mathbf{r}_\parallel)$, essentially. The contribution to this difference from the $\mathbf{k}_\parallel$ component is proportional to

$$|\psi^T(\mathbf{r}_\parallel;\mathbf{k}_\parallel)|^2 - \left|\psi^\infty_{\mathbf{k}_\parallel}(\mathbf{r}_\parallel)\right|^2 = |\psi^S(\mathbf{r}_\parallel;\mathbf{k}_\parallel)|^2 + \left[\left(\psi^\infty_{\mathbf{k}_\parallel}(\mathbf{r}_\parallel)\right)^* \psi^S(\mathbf{r}_\parallel;\mathbf{k}_\parallel) + \text{C.c.}\right]. \tag{86}$$

The range of this difference is given by the term proportional to $\psi^S(\mathbf{r}_\parallel;\mathbf{k}_\parallel)[(\psi^S(\mathbf{r}_\parallel;\mathbf{k}_\parallel))^*]$ and, hence, by the range of the Hankel function $H_0^{(1)}(k_\parallel|\mathbf{r}_\parallel - \mathbf{r}'_\parallel|)$; i.e., $(k_\parallel|\mathbf{r}_\parallel - \mathbf{r}'_\parallel|)^{-1/2}$.

APPENDIX A: NOTES ON THE APERTURE-FIELD CALCULATION

It is not the purpose of this Appendix to present a review of the method by which the introduction of a *fictitious* magnetic current density distribution in the aperture region may allow one to determine the aperture field $\boldsymbol{\mathcal{E}}(\mathbf{r}_\parallel)$ in Eq. (19). However, the notes given below may be useful seen from the perspective of our microscopic theory.

Let us assume that we have a *magnetic* (sheet) current density distribution $\mathbf{J}^M_\parallel(\mathbf{r}_\parallel;\omega) = \mathbf{J}^M_\parallel(\mathbf{r}_\parallel)$ in the aperture region and that this, as indicated by the notation, has no component perpendicular to the plane of the screen (similar to the general assumption for the electric current density in classical diffraction theory). In the magnetic Lorenz gauge the (scattered) magnetic vector potential, $\mathbf{a}^S$, originating in this sheet current density, then is given by

$$\mathbf{a}^S(\mathbf{r}_\parallel) = \mu_0 \int_{\mathcal{A}} g(|\mathbf{r}_\parallel - \mathbf{r}'_\parallel|)\mathbf{J}^M_\parallel(\mathbf{r}'_\parallel) d^2 r'_\parallel \tag{A1}$$

at the arbitrary point $\mathbf{r}_\parallel = (x,y)$ inside the aperture [cf. Eq. (10)]. Although $g(|\mathbf{r}_\parallel - \mathbf{r}'_\parallel|)$ is singular at $\mathbf{r}'_\parallel = \mathbf{r}_\parallel$, the integral in Eq. (A1) is absolutely convergent. To obtain the magnetic vector potential [$\mathbf{a}^S(\mathbf{r})$] also outside the aperture plane, one just makes the replacement $\mathbf{r}_\parallel \Rightarrow \mathbf{r}$ in Eq. (A1). Knowledge of $\mathbf{a}^S(\mathbf{r})$ allows one to obtain the scattered electric and magnetic fields from

$$\mathbf{E}^S(\mathbf{r}) = -c\nabla \times \mathbf{a}^S(\mathbf{r}) \tag{A2}$$

and

$$\mathbf{B}^S(\mathbf{r}) = iq_0 \mathbf{a}^S(\mathbf{r}) + \frac{i}{q_0}\nabla\nabla \cdot \mathbf{a}^S(\mathbf{r}), \tag{A3}$$

remembering that

$$a^S_\perp(\mathbf{r}) = 0. \tag{A4}$$

The electromagnetic field defined by Eqs. (A1) (with $\mathbf{r}_\parallel \Rightarrow \mathbf{r}$) to (A4) satisfies the Maxwell equations for $z \neq 0$ and the boundary conditions at our perfect metal screen [$\mathbf{E}_\parallel = \mathbf{0}$ and $B_\perp = 0$].

From $\nabla \cdot \mathbf{E} = 0$ it follows that $E_\perp(\mathbf{r}_\parallel,0^+) = E_\perp(\mathbf{r}_\parallel,0^-)$, and since $E_\perp = 0$ (and also $\mathbf{E}_\parallel = \mathbf{0}$) inside our *perfect* magnetic conductor (a perfect magnetic conductor assumption is a necessity in order to fulfill the boundary conditions), one realizes that

$$E^0_\perp(\mathbf{r}_\parallel) + E^S_\perp(\mathbf{r}_\parallel) = 0 \tag{A5}$$

in the aperture ($z = 0$). By means of Eq. (A2) taken for $\mathbf{r} = \mathbf{r}_\parallel$, the condition in Eq. (A5) can be rewritten in the form

$$\frac{\partial}{\partial x} a^S_y(\mathbf{r}_\parallel) - \frac{\partial}{\partial y} a^S_x(\mathbf{r}_\parallel) = \frac{1}{c} E^0_\perp(\mathbf{r}_\parallel). \tag{A6}$$

For a perfect magnetic conductor one, finally, must have

$$\mathbf{B}^0_\parallel(\mathbf{r}_\parallel) + \mathbf{B}^S_\parallel(\mathbf{r}_\parallel) = \mathbf{0}, \tag{A7}$$

in analogy to the circumstance that $\mathbf{E}_\parallel = \mathbf{0}$ (and also $\mathbf{E} = \mathbf{0}$) in a perfect electric conductor. If one utilizes Eqs. (A3) and (A6) and remembers that the incident field must satisfy the dual Maxwell equation $-\nabla \times \mathbf{E}^0 = -i\omega \mathbf{B}^0$ (no source term), some algebraic effort allows one to rewrite Eq. (A7) as

$$\left(\nabla^2_\parallel + q_0^2\right)\mathbf{a}^S(\mathbf{r}_\parallel) = \frac{1}{c}\hat{\mathbf{n}} \times \left[\frac{\partial}{\partial z}\mathbf{E}^0_\parallel(\mathbf{r}_\parallel,z)\right]_{z=0}. \tag{A8}$$

The set of complicated differential-integral equations in Eqs. (A1), (A6), and (A8), is the starting point for the determination of $\mathbf{J}^M_\parallel(\mathbf{r}_\parallel)$ and, subsequently, $\hat{\mathbf{n}} \times \boldsymbol{\mathcal{E}}(\mathbf{r}_\parallel)$, given $E^0_\perp$ and $\partial \mathbf{E}^0_\parallel / \partial z$ in the aperture region. These equations also are those used by Bouwkamp in his critical analysis of Bethe's theory [7,9].

In the Bethe-Bouwkamp theory it is assumed that the metallic part of the screen is opaque (a perfect conductor). If such a drastic assumption is made for all frequencies in the

microscopic approach, Eq. (57) is reduced to

$$\mathbf{E}(\mathbf{r},\omega) = \mathbf{E}_\infty(\mathbf{r},\omega) + \mathbf{E}^{\mathcal{A}}(\mathbf{r},\omega), \quad z < 0, \tag{A9}$$

$$\mathbf{E}(\mathbf{r},\omega) = \mathbf{E}^{\mathcal{A}}(\mathbf{r},\omega), \quad z > 0, \tag{A10}$$

since $\mathbf{E}_\infty(\mathbf{r},\omega) = \mathbf{0}$ in the half-space $z > 0$. The reflection symmetry of the aperture field in the $z = 0$ plane is determined by the related symmetry of the dyadic Green function, $\mathbf{G}(|\mathbf{r}_\parallel - \mathbf{r}'_\parallel|,z;\omega)$ [see Eqs. (55) and (63)]. It is known (see Ref. [59]) that the Green function in the mixed representation has the tensorial form

$$\mathbf{G}(|\mathbf{r}_\parallel - \mathbf{r}'_\parallel|,z) = \begin{pmatrix} G_{xx} & 0 & G_{xz} \\ 0 & G_{yy} & 0 \\ G_{zx} & 0 & G_{zz} \end{pmatrix}. \tag{A11}$$

If one only allows the sheet current to flow in the plane of the screen (the assumption of the classical diffraction theory), the symmetries of $\mathbf{E}^{\mathcal{A}}_\parallel$'s x and y components are those of G_{xx} and G_{yy}. Since these are symmetric in z, $\mathbf{E}^{\mathcal{A}}_\parallel(\mathbf{r}_\parallel,z) = \mathbf{E}^{\mathcal{A}}_\parallel(\mathbf{r}_\parallel,-z)$. The normal component $E^{\mathcal{A}}_\perp$ has the odd reflection symmetry of G_{zx}; that is, $\mathbf{E}^{\mathcal{A}}_\parallel(\mathbf{r}_\parallel,z) = -\mathbf{E}^{\mathcal{A}}_\parallel(\mathbf{r}_\parallel,-z)$. The symmetries of the microscopic aperture field with the assumption that $\mathbf{J}_\perp = 0$ hence are in agreement with those of Bethe; see Eqs. (7), (9), and (9c) in Ref. [7].

APPENDIX B: GENERALIZED JUMP CONDITIONS

As mentioned in Sec. II B, classical diffraction theory makes use of the assumption that the sheet current density, $\mathbf{J}^S(\mathbf{r}_\parallel)$, has no component perpendicular to the plane of the screen; that is, $J^S_\perp(\mathbf{r}_\parallel)[\equiv J^S_z(\mathbf{r}_\parallel)] = 0$. However, it is known that the assumption cannot be correct in general [cf. the remarks following Eq. (10)]. When $J^S_\perp(\mathbf{r}_\parallel)$ is nonvanishing the standard (textbook) boundary condition, which asserts that the vectorial component ($\mathbf{E}_\parallel$) of the electric field parallel to the given sharp interface is continuous, must be modified. In the present context this means that $\mathbf{E}_\parallel$ suffers a finite jump ($\Delta\mathbf{E}_\parallel$) across the sheet.

1. Generalization of the result of Ref. [34] for $\Delta\mathbf{E}_\parallel$

In the sheet model description of the linear optical response of a QW given in Ref. [34], it was concluded (see Eqs. (91) and (94) in Ref. [34]) that

$$\mathbf{E}_\parallel(q_\parallel\hat{\mathbf{x}};z=0^+) - \mathbf{E}_\parallel(q_\parallel\hat{\mathbf{x}};z=0^-) = \frac{q_\parallel\hat{\mathbf{x}}}{\varepsilon_0\omega} J^S_\perp(q_\parallel\hat{\mathbf{x}}) \tag{B1}$$

in the mixed representation and for $\mathbf{q}_\parallel = q_\parallel\hat{\mathbf{x}}$. Since the result for the jump cannot depend on the orientation of the Cartesian axes perpendicular to $\hat{\mathbf{z}}$, it follows that

$$\mathbf{E}_\parallel(\mathbf{q}_\parallel;0^+) - \mathbf{E}_\parallel(\mathbf{q}_\parallel;0^-) = \frac{\mathbf{q}_\parallel}{\varepsilon_0\omega} J^S_\perp(\mathbf{q}_\parallel) \tag{B2}$$

in the general case where $\mathbf{q}_\parallel = q_{\parallel,x}\hat{\mathbf{x}} + q_{\parallel,y}\hat{\mathbf{y}}$. A 2D Fourier-integral transformation of Eq. (B2) immediately leads to the following jump condition in direct space:

$$\mathbf{E}_\parallel(\mathbf{r}_\parallel,0^+) - \mathbf{E}_\parallel(\mathbf{r}_\parallel,0^-) = \frac{1}{i\varepsilon_0\omega}\nabla_\parallel J^S_\perp(\mathbf{r}_\parallel). \tag{B3}$$

The result in Eq. (B3) is in agreement with the jump obtained for the parallel component of the aperture field ($\mathbf{E}^{\mathcal{A}}_\parallel$) on the basis of the Green function in disk contraction [see Eq. (68)].

2. Alternative derivation of the jump in $\mathbf{E}_\parallel$

Additional insight into the physics hidden in Eq. (B3) may be obtained by the derivation presented below. Studying the alternative calculation, the reader need not to be familiar with the derivation given in Ref. [34].

From the microscopic Maxwell-Lorentz equation

$$\nabla \times \mathbf{B}(\mathbf{r};\omega) = \mu_0\mathbf{J}(\mathbf{r};\omega) - \frac{i\omega}{c_0^2}\mathbf{E}(\mathbf{r};\omega), \tag{B4}$$

it appears that rotational-free [often called longitudinal (L)] parts of the electric field ($\mathbf{E}_L$) and the current density ($\mathbf{J}_L$) are related by

$$\mathbf{J}_L(\mathbf{r};\omega) = i\varepsilon_0\omega\mathbf{E}_L(\mathbf{r};\omega). \tag{B5}$$

Furthermore, $\mathbf{J}_L$ is related to the current density itself, $\mathbf{J}$, by a spatially nonlocal relation which, in the mixed representation, takes the form (omitting the reference to ω)

$$\mathbf{J}_L(\mathbf{q}_\parallel;z) = \int_{-\infty}^{\infty} \boldsymbol{\delta}_L(\mathbf{q}_\parallel,z-z')\cdot\mathbf{J}(\mathbf{q}_\parallel,z')dz', \tag{B6}$$

where (with $z - z' = Z$ and $\hat{\mathbf{q}}_\parallel = \mathbf{q}_\parallel/q_\parallel$)

$$\boldsymbol{\delta}_L(\mathbf{q}_\parallel,Z) = \hat{\mathbf{z}}\hat{\mathbf{z}}\delta(Z) + \frac{q_\parallel}{2}e^{-q_\parallel|Z|} \times [\hat{\mathbf{q}}_\parallel\hat{\mathbf{q}}_\parallel - \hat{\mathbf{z}}\hat{\mathbf{z}} + i(\hat{\mathbf{q}}_\parallel\hat{\mathbf{z}} + \hat{\mathbf{z}}\hat{\mathbf{q}}_\parallel)\mathrm{sgn}(Z)] \tag{B7}$$

is the dyadic longitudinal δ function in disk contraction [50]. For z coordinates *inside* a QW (screen) of *finite thickness*, one thus has

$$\mathbf{J}_L(\mathbf{q}_\parallel;z) = \hat{\mathbf{z}}J_\perp(\mathbf{q}_\parallel;z) + (\ldots), \tag{B8}$$

where $(\ldots)$ is the nonlocal contribution originating in the second line of Eq. (B7). When the QW thickness tends to 0, the term $\hat{\mathbf{z}}J_\perp(\mathbf{q}_\parallel;z)$ will be the dominating part of the right-hand side of Eq. (B8) ($\hat{\mathbf{z}}J_\perp$ develops into a δ function singularity, whereas the nonlocal term stays finite). With

$$\mathbf{J}_L(\mathbf{q}_\parallel;z) \approx J_\perp(\mathbf{q}_\parallel;z)\hat{\mathbf{z}} = J^S_\perp(\mathbf{q}_\parallel)\delta(z)\hat{\mathbf{z}}, \tag{B9}$$

the longitudinal electric field is given by

$$\mathbf{E}_L(\mathbf{q}_\parallel;z) = \frac{1}{i\varepsilon_0\omega}J^S_\perp(\mathbf{q}_\parallel)\delta(z)\hat{\mathbf{z}} \tag{B10}$$

in the mixed representation. From the physical point of view it is intuitively clear that the jump conditions for the electric field across a QW of thickness much smaller than the wavelength of the electromagnetic field may be calculated retaining only the nonretarded longitudinal part of the electric field. With $\mathbf{E} \approx \mathbf{E}_L$,

$$\nabla \times \mathbf{E}(\mathbf{r}_\parallel,z) \simeq \mathbf{0}, \tag{B11}$$

and upon a 2D Fourier transformation of Eq. (B10),

$$\mathbf{E}(\mathbf{r}_\parallel,z) \simeq \frac{1}{i\varepsilon_0\omega}J^S_\perp(\mathbf{r}_\parallel)\delta(z)\hat{\mathbf{z}}. \tag{B12}$$

Together Eqs. (B11) and (B12) allow one to regain the jump condition in Eq. (B3). To realize this, let us integrate the y component of Eq. (B11) from $z = 0^-$ to 0^+ keeping $\mathbf{r}_\parallel$ fixed. Thus,

$$\int_{0^-}^{0^+} \frac{\partial}{\partial z} E_x(\mathbf{r}_\parallel,z)dz = \int_{0^-}^{0^+} \frac{\partial}{\partial x} E_z(\mathbf{r}_\parallel,z)dz, \tag{B13}$$

and then

$$E_x(\mathbf{r}_\parallel,0^+) - E_x(\mathbf{r}_\parallel,0^-) = \frac{\partial}{\partial x} \int_{0^-}^{0^+} E_z(\mathbf{r}_\parallel,z)dz. \tag{B14}$$

By inserting the expression for $E_z(\mathbf{r}_\parallel,z)$ given in Eq. (B12) under the integral sign in Eq. (B14), one obtains

$$E_x(\mathbf{r}_\parallel,0^+) - E_x(\mathbf{r}_\parallel,0^-) = \frac{1}{i\varepsilon_0\omega} \frac{\partial}{\partial x} J_\perp^S(\mathbf{r}_\parallel). \tag{B15}$$

A similar derivation, via the x component of Eq. (B11), leads to

$$E_y(\mathbf{r}_\parallel,0^+) - E_y(\mathbf{r}_\parallel,0^-) = \frac{1}{i\varepsilon_0\omega} \frac{\partial}{\partial y} J_\perp^S(\mathbf{r}_\parallel). \tag{B16}$$

The results of Eqs. (B15) and (B16) are precisely the x and the y component of Eq. (B3). QED.

3. The jump in $E_\perp$

To obtain the jump condition for the z component of the electric field, $E_z(\mathbf{r};\omega) \equiv E_\perp(\mathbf{r};\omega)$, by integration across the sheet, we start from the Maxwell-Lorentz equation

$$\nabla \cdot \mathbf{E}(\mathbf{r};\omega) = \varepsilon_0^{-1} \rho(\mathbf{r};\omega), \tag{B17}$$

where $\rho(\mathbf{r};\omega)$ is the microscopic charge density. Hence,

$$\int_{0^-}^{0^+} \frac{\partial}{\partial z} E_\perp(\mathbf{r}_\parallel,z)dz = \frac{1}{\varepsilon_0} \int_{0^-}^{0^+} \rho(\mathbf{r}_\parallel,z)dz - \nabla_\parallel \cdot \int_{0^-}^{0^+} \mathbf{E}_\parallel(\mathbf{r}_\parallel,z)dz. \tag{B18}$$

Since $\mathbf{E}_\parallel$ is finite throughout the QW, the last term in Eq. (B18) vanishes when the sheet becomes infinitely thin. This fact is in line with the circumstance that only the longitudinal part of $\mathbf{E}$ enters Eq. (B17) ($\nabla \cdot \mathbf{E}_T = 0$) and that this part in turn tends to be directed perpendicular to the QW plane when the sheet thickness goes to 0. Consequently, one obtains

$$E_\perp(\mathbf{r}_\parallel,0^+) - E_\perp(\mathbf{r}_\parallel,0^-) = \varepsilon_0^{-1} \rho^S(\mathbf{r}_\parallel), \tag{B19}$$

where

$$\rho^S(\mathbf{r}_\parallel) = \int_{0^-}^{0^+} \rho(\mathbf{r}_\parallel,z)dz \tag{B20}$$

is the ED-ED sheet charge density. By employing the 2D version of the charge equation of continuity, viz.,

$$\nabla_\parallel \cdot \mathbf{J}_\parallel^S(\mathbf{r}_\parallel;\omega) = i\omega\rho^S(\mathbf{r}_\parallel;\omega), \tag{B21}$$

Eq. (B19) may be written as

$$E_\perp(\mathbf{r}_\parallel,0^+) - E_\perp(\mathbf{r}_\parallel,0^-) = \frac{1}{i\varepsilon_0\omega} \nabla_\parallel \cdot \mathbf{J}_\parallel^S(\mathbf{r}_\parallel), \tag{B22}$$

a result identical to the form given for the aperture field jump in Eq. (69).

4. The jump in $\mathbf{B}_\parallel$

It is instructive to apply the method presented in Sec. B 2 to obtain the jump in the vectorial component of the microscopic magnetic field parallel to the sheet plane. With $\mathbf{E} \simeq \mathbf{E}_L$, the divergence-free [transverse (T)] part of Eq. (B4) takes the approximate form

$$\nabla \times \mathbf{B}(\mathbf{r};\omega) = \mu_0 \mathbf{J}_T(\mathbf{r};\omega). \tag{B23}$$

Following the argumentation in Sec. B 2, it is obvious that the transverse current density, $\mathbf{J}_T = \mathbf{J} - \mathbf{J}_L$, may be approximated by the self-field form

$$\mathbf{J}_T(\mathbf{r}) = (\mathbf{U} - \hat{\mathbf{z}}\hat{\mathbf{z}}) \cdot \mathbf{J}(\mathbf{r}) \tag{B24}$$

when the QW thickness tends toward 0 [cf. Eq. (B9)]. From Eq. (B24) one then sees that the direction of $\mathbf{J}_T(\mathbf{r})$ becomes parallel to the sheet plane; i.e.,

$$\mathbf{J}_T(\mathbf{r}) \simeq \mathbf{J}_\parallel(\mathbf{r}). \tag{B25}$$

An integration of the x component of Eq. (B23) across the sheet with Eq. (B25) inserted now gives

$$B_y(\mathbf{r}_\parallel,0^+) - B_y(\mathbf{r}_\parallel,0^-) = \frac{\partial}{\partial y} \int_{0^-}^{0^+} B_z(\mathbf{r}_\parallel,z)dz - \mu_0 \int_{0^-}^{0^+} J_{\parallel,x}(\mathbf{r}_\parallel,z)dz. \tag{B26}$$

The first term on the right-hand side of Eq. (B26) vanishes in the limit since B_z stays finite. The jump therefore is given by

$$B_y(\mathbf{r}_\parallel,0^+) - B_y(\mathbf{r}_\parallel,0^-) = -\mu_0 J_{\parallel,x}^S(\mathbf{r}_\parallel). \tag{B27}$$

An analogous expression can be derived for the jump in B_x, and together the two jump conditions may be written in the well-known compact vectorial form

$$\hat{\mathbf{n}} \times (\mathbf{B}(\mathbf{r}_\parallel,0^+) - \mathbf{B}(\mathbf{r}_\parallel,0^-)) = \mu_0 \mathbf{J}_\parallel^S(\mathbf{r}_\parallel). \tag{B28}$$

The last "jump" condition,

$$\hat{\mathbf{n}} \cdot (\mathbf{B}(\mathbf{r}_\parallel,0^+) - \mathbf{B}(\mathbf{r}_\parallel,0^-)) = 0, \tag{B29}$$

expressing the continuity in the normal component of the magnetic field is of no concern here.

In the microscopic approach only $\mathbf{E}$ and $\mathbf{B}$ fields occur, and *all* "dielectric" and "magnetic" properties are contained in the microscopic conductivity response tensor (see Ref. [42], and references therein). For this reason it is of no use to introduce auxiliary $\mathbf{D}$ and $\mathbf{H}$ fields in our approach (Sec. III). However, in classical diffraction theory (Sec. II) it is important to specify the permittivity and permeability properties of the media in question, of course.

APPENDIX C: FIELD ASYMMETRIES WHEN $\mathbf{J}_\perp^S(\mathbf{r}_\parallel;\omega) \neq \mathbf{0}$

In classical diffraction theory the scattered electric and magnetic fields from an infinitely thin screen, *assumed* to be able to carry a frequency-dependent current density only parallel to the plane ($z = 0$) of the screen, satisfy certain

well-known reflection symmetries in z; i.e., $\mathbf{E}_\parallel^S$ and $B_\perp^S$ are even and $E_\perp^S$ and $\mathbf{B}_\parallel^S$ are odd [6]. In the general case, where the sheet current density also has a component $\mathbf{J}_\perp^S(\mathbf{r}_\parallel;\omega)$, perpendicular to the plane of the screen, some of the reflection properties of the fields are modified.

To obtain the new asymmetric reflection properties we start from the integral expression

$$\mathbf{A}^S(\mathbf{r};\omega) = \mu_0 \int_S g(|\mathbf{r}-\mathbf{r}'_\parallel|;\omega)\mathbf{J}^S(\mathbf{r}'_\parallel;\omega)d^2r'_\parallel, \tag{C1}$$

giving the scattered vector potential from an ED-ED current density sheet in the Lorenz gauge. It appears from Eq. (C1) that $\mathbf{A}^S$ is even in z; i.e.,

$$\mathbf{A}^S(\mathbf{r}_\parallel,-z) = \mathbf{A}^S(\mathbf{r}_\parallel,z). \tag{C2}$$

The reflection properties of the scattered magnetic field are determined from Eq. (29) utilizing the symmetry in Eq. (C2). As the reader may show, one obtains

$$B_\perp^S(\mathbf{r}_\parallel,-z) = B_\perp^S(\mathbf{r}_\parallel,z) \tag{C3}$$

and

$$\begin{aligned}&\hat{\mathbf{n}}\times(\mathbf{B}_\parallel^S(\mathbf{r}_\parallel,z)+\mathbf{B}_\parallel^S(\mathbf{r}_\parallel,-z))\\ &\quad= 2\nabla_\parallel A_\perp^S(\mathbf{r}_\parallel,z) = 2\nabla_\parallel\int_S g(|\mathbf{r}-\mathbf{r}'_\parallel|)J_\perp^S(\mathbf{r}'_\parallel)d^2r'_\parallel.\end{aligned} \tag{C4}$$

It appears from Eqs. (C3) and (C4) that only the symmetry of the parallel component of the scattered magnetic field is modified: When $J_\perp^S \neq 0$, $\mathbf{B}_\parallel^S$ is no longer odd in z. By combining Eqs. (B28) and (C4) one obtains the result in Eq. (11) for $J_\perp^S = 0$.

The reflection properties of the scattered electric field are determined utilizing Eq. (C2) in the Lorenz gauge connection given in Eq. (30). Thus, it is realized that

$$\begin{aligned}&\mathbf{E}_\parallel^S(\mathbf{r}_\parallel,z)-\mathbf{E}_\parallel^S(\mathbf{r}_\parallel,-z)\\ &\quad= 2i\omega q_0^{-2}\nabla_\parallel\frac{\partial}{\partial z}A_\perp(\mathbf{r}_\parallel,z)\\ &\quad= 2i\omega q_0^{-2}\nabla_\parallel\frac{\partial}{\partial z}\int_S g(|\mathbf{r}-\mathbf{r}'_\parallel|)J_\perp^S(\mathbf{r}'_\parallel)d^2r'_\parallel\end{aligned} \tag{C5}$$

and

$$\begin{aligned}&E_\perp^S(\mathbf{r}_\parallel,z)+E_\perp^S(\mathbf{r}_\parallel,-z)\\ &\quad= 2i\omega\left[1+q_0^{-2}\frac{\partial^2}{\partial z^2}\right]A_\perp^S(\mathbf{r}_\parallel,z)\\ &\quad= 2i\omega\left[1+q_0^{-2}\frac{\partial^2}{\partial z^2}\right]\int_S g(|\mathbf{r}_\parallel-\mathbf{r}'_\parallel|)J_\perp^S(\mathbf{r}'_\parallel)d^2r'_\parallel.\end{aligned} \tag{C6}$$

Hence, the symmetries of both the parallel and the perpendicular components of the scattered electric field are modified when $J_\perp^S \neq 0$. However, note that the standard reflection symmetries [6] in z are recovered from Eqs. (C3)–(C6) if $J_\perp^S = 0$.

In order to investigate the correspondence between the microscopic and the macroscopic diffraction theories it would be important to modify the standard theory of classical diffraction so as to account for situations where $J_\perp^S \neq 0$. Such a modification, which is outside the scope of the present study, would require the use of the reflection properties given in Eqs. (C2)–(C6), as well as the generalized jump conditions presented in Appendix B.

We end this Appendix with a figure presenting a schematic overview of the derived reflection properties [Eqs. (C2)–(C6)] and jumps [Eqs. (B3), (B22), (B28), and (B29)] of the electromagnetic field across an ED-ED current density sheet (Fig. 6). The figure also presents a comparison with the usual textbook results, where the assumption $J_\perp^S = 0$ is imposed.

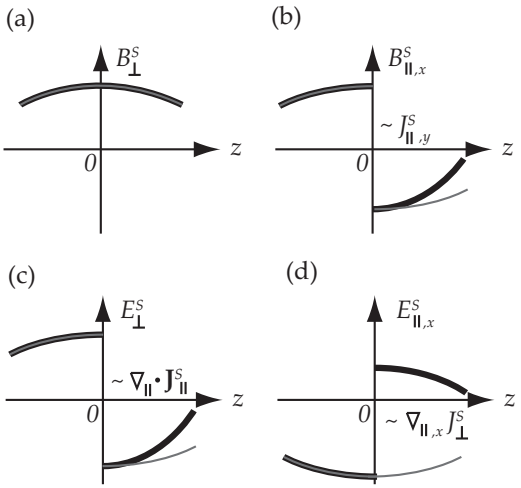

FIG. 6. Schematics of the asymmetries and jumps in the various electromagnetic field components (thick black lines) across a current sheet placed at $z = 0$. The usual textbook result, with the assumption $J_\perp^S = 0$, is also sketched (thin gray lines). (a) The symmetry and the jump in $B_\perp^S$ are the same in the two cases. (b) The jump in $\mathbf{B}_\parallel$ (only the x component is shown here) is the same, but the symmetry is no longer antisymmetric with respect to z. (c) The jump in $E_\perp$ is the same, but the symmetry is modified; it is no longer antisymmetric with respect to z. (d) Both the jump and the symmetry of $\mathbf{E}_\parallel$ (only the x component is sketched here) are modified. In the general case $\mathbf{E}_\parallel$ jumps at $z = 0$ and it is not symmetric with respect to z. Note also that the jumps in $\mathbf{B}_\parallel$ and $E_\perp$ in general are not symmetric around 0 [as depicted in (b) and (c)]. For the textbook case where $J_\perp^S = 0$ this is a condition imposed by the antisymmetry of $\mathbf{B}_\parallel$ and $E_\perp$. This antisymmetry is lost for $J_\perp^S \neq 0$. An alternative sketch of the x component of $\mathbf{B}_\parallel$ is shown in Fig. 7.

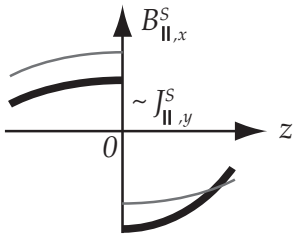

FIG. 7. Alternative sketch of the x component of $\mathbf{B}_\parallel$. As in Fig. 6, thick black lines are the generalized case with $J_\perp^S \neq 0$ and thin gray lines represent the textbook result in which $J_\perp^S = 0$.

[1] M. Born and E. Wolf, *Principles of Optics: Electromagnetic Theory of Propagation, Interference and Diffraction of Light*, 7th ed. (Cambridge University Press, Cambridge, 1999).
[2] H. von Helmholtz, J. f. Math. **57**, 7 (1859).
[3] G. Kirchhoff, Berl. Ber. 641 (1882).
[4] G. Kirchhoff, Wied. Ann. **18**, 663 (1883).
[5] J. A. Stratton, *Electromagnetic Theory*, 1st ed. (McGraw–Hill, New York, 1941).
[6] J. D. Jackson, *Classical Electrodynamics*, 3rd ed. (Wiley, New York, 1999).
[7] H. A. Bethe, Phys. Rev. **66**, 163 (1944).
[8] C. J. Bouwkamp, Philips Res. Rep. **5**, 321 (1950).
[9] C. J. Bouwkamp, Rep. Prog. Phys. **17**, 35 (1954).
[10] A. Lewis, M. Isaacson, A. Harootunian, and A. Muray, Ultramicroscopy **13**, 227 (1984).
[11] D. W. Pohl, W. Denk, and M. Lanz, Appl. Phys. Lett. **44**, 651 (1984).
[12] T. W. Ebbesen, H. J. Lezec, H. F. Ghaemi, T. Thio, and P. A. Wolff, Nature **391**, 667 (1998).
[13] C. Genet and T. W. Ebbesen, Nature **445**, 39 (2007).
[14] H. Liu and P. Lalanne, Nature **452**, 728 (2008).
[15] F. J. Garcia-Vidal, L. Martin-Moreno, T. W. Ebbesen, and L. Kuipers, Rev. Mod. Phys. **82**, 729 (2010).
[16] A. Roberts, J. Opt. Soc. Am. A, **4**, 1970 (1987).
[17] F. J. G. de Abajo, Opt. Express **10**, 1475 (2002).
[18] F. J. Garcia-Vidal, E. Moreno, J. A. Porto, and L. Martin-Moreno, Phys. Rev. Lett. **95**, 103901 (2005).
[19] A. Y. Nikitin, D. Zueco, F. J. Garcia-Vidal, and L. Martin-Moreno, Phys. Rev. B **78**, 165429 (2008).
[20] S. Carretero-Palacios, F. J. Garcia-Vidal, L. Martin-Moreno, and S. G. Rodrigo, Phys. Rev. B **85**, 035417 (2012).
[21] R. Wannemacher, Opt. Commun. **195**, 107 (2001).
[22] G. C. des Francs, D. Molenda, U. C. Fischer, and A. Naber, Phys. Rev. B **72**, 165111 (2005).
[23] B. Sepulveda, Y. Alaverdyan, J. Alegret, M. Käll, and P. Johansson, Opt. Express **16**, 5609 (2008).
[24] O. J. F. Martin, C. Girard, and A. Dereux, Phys. Rev. Lett. **74**, 526 (1995).
[25] A. Y. Nikitin, F. J. Garcia-Vidal, and L. Martin-Moreno, Phys. Rev. Lett. **105**, 073902 (2010).
[26] I. Fernandez-Corbaton, N. Tischler, and G. Molina-Terriza, Phys. Rev. A **84**, 053821 (2011).
[27] S.-H. Chang, S. K. Gray, and G. C. Schatz, Opt. Express **13**, 3150 (2005).
[28] V. G. Bordo, Phys. Rev. B **84**, 075465 (2011).
[29] O. Keller, Phys. Rev. A **60**, 1652 (1999).
[30] O. Keller, *Light—The Physics of the Photon*, 1st ed. (CRC, Taylor & Francis, London, 2014).
[31] M. O. Scully and K. Drühl, Phys. Rev. A **25**, 2208 (1982).
[32] M. O. Scully and M. S. Zubairy, *Quantum Optics* (Cambridge University Press, Cambridge, 1997).
[33] W. R. Smythe, Phys. Rev. **72**, 1066 (1947).
[34] O. Keller, J. Opt. Soc. Am. B **12**, 987 (1995).
[35] O. Keller, J. Opt. Soc. Am. B **12**, 997 (1995).
[36] J. Jung and O. Keller (unpublished).
[37] M. V. Klein and T. E. Furtak, *Optics*, 2nd ed. (Wiley, New York, 1986).
[38] L. Lorenz, Ann. Phys. (Pogg.) **111**, 315 (1860).
[39] L. Lorenz, Skand. Naturf. Förh. **8**, 473 (1860).
[40] O. Keller, in *Progress in Optics, Vol. 43*, edited by E. Wolf (Elsevier, Amsterdam, 2002), p. 195.
[41] L. Rayleigh, Philos. Mag. **43**, 259 (1897).
[42] O. Keller, *Quantum Theory of Near-Field Electrodynamics* (Springer, Berlin, 2011).
[43] F. Kottler, in *Progress in Optics, Vol. 4*, edited by E. Wolf (Elsevier, Amsterdam, 1965), p. 281.
[44] F. Kottler, in *Progress in Optics, Vol. 6*, edited by E. Wolf (Elsevier, Amsterdam, 1967), p. 331.
[45] L. Novotny and B. Hecht, *Principles of Nano-Optics*, 1st ed. (Cambridge University Press, Cambridge, 2006).
[46] D. Bohm and D. Pines, Phys. Rev. **82**, 625 (1951); D. Pines and D. Bohm, *ibid.* **85**, 338 (1952); D. Bohm and D. Pines, *ibid.* **92**, 609 (1953); D. Pines, *ibid.* **92**, 626 (1953).
[47] G. D. Mahan, *Many-Particle Physics* (Plenum Press, New York, 1990).
[48] O. Keller, Phys. Rev. B **34**, 3883 (1986).
[49] O. Keller, Phys. Rev. B **37**, 10588 (1988).
[50] O. Keller, in *Progress in Optics, Vol. 37*, edited by E. Wolf (Elsevier, Amsterdam, 1997), p. 257.
[51] C. Obermuller and K. Karrai, Appl. Phys. Lett. **67**, 3408 (1995).
[52] A. Degiron, H. J. Lezec, N. Yamamoto, and T. W. Ebbesen, Opt. Commun. **239**, 61 (2004).
[53] J. Prikulis, P. Hanarp, L. Olofsson, D. Sutherland, and M. Käll, Nano Lett. **4**, 1003 (2004).
[54] T. Rindzevicius, Y. Alaverdyan, B. Sepulveda, T. Pakizeh, M. Käll, R. Hillenbrand, J. Aizpurua, and F. J. G. de Abajo, J. Phys. Chem. C **111**, 1207 (2007).
[55] A. J. L. Adam, J. M. Brok, M. A. Seo, K. J. Ahn, D. S. Kim, J. H. Kang, Q. H. Park, M. Nagel, and P. C. M. Planken, Opt. Express **16**, 7407 (2008).
[56] T.-H. Park, N. Mirin, J. B. Lassiter, C. L. Nehl, N. J. Halas, and P. Nordlander, ACS Nano **2**, 25 (2008).
[57] O. Keller, Phys. Rep. **268**, 85 (1996).
[58] P. J. Feibelman, Prog. Surf. Sci. **12**, 287 (1982).
[59] O. Keller, J. Opt. Soc. Am. B **16**, 835 (1999).